ISSN : 0973-0613

JOURNAL OF Wind and Engineering

Vol. 8 No.1 January 2011

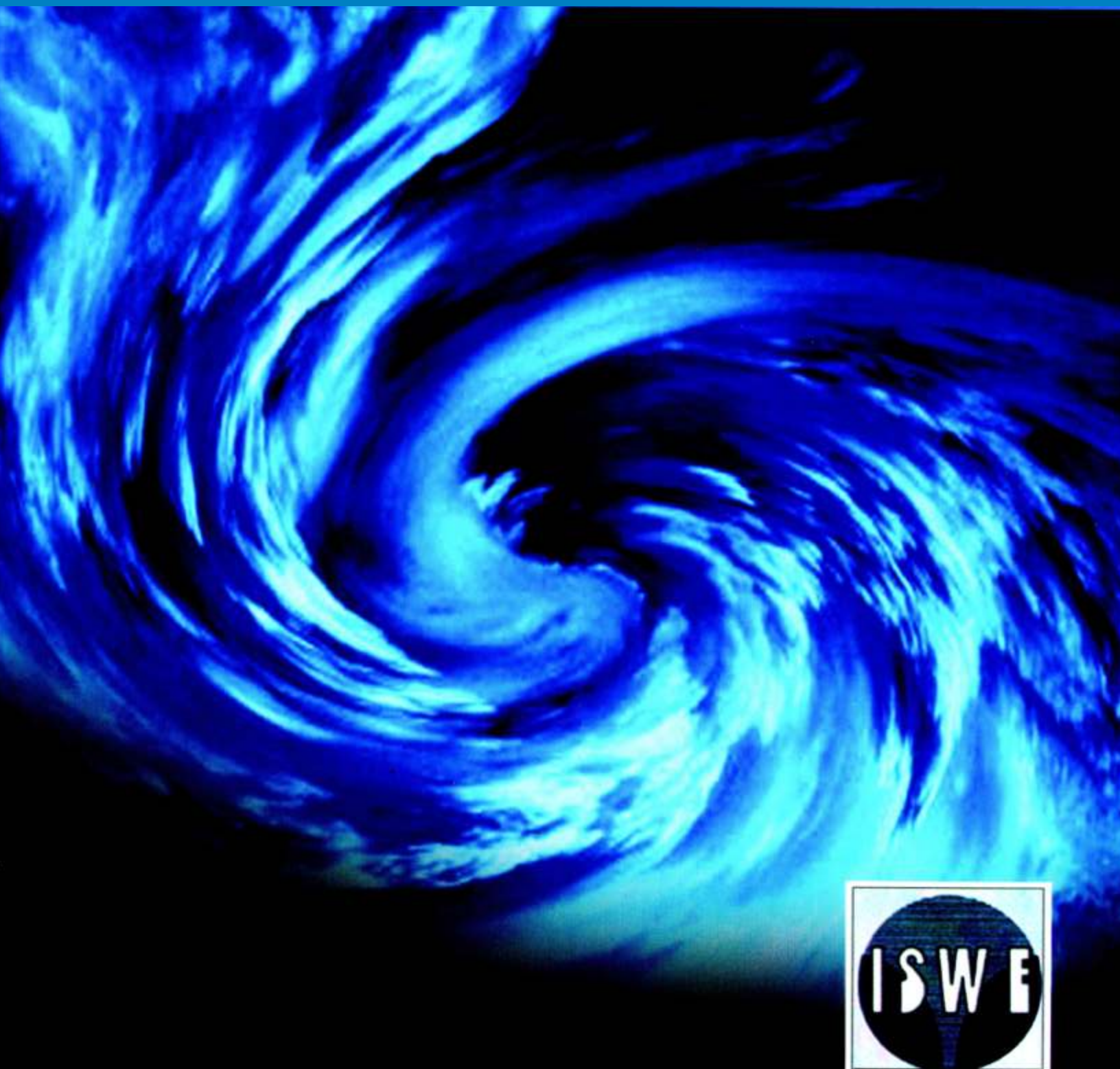

ISWE

Journal of Wind and Engineering

Editor-in-Chief

Editors

International Review Board

JOURNAL OF WIND & ENGINEERING

Vol. 8 No. 1 January 2011

CONTENTS

Journal of Wind and Engineering, Vol. 8, No. 1, January 2011, PP. 1-9

WIND RESPONSE CONTROL OF TALL RC CHIMNEYS

K.R.C. Reddy[1] , O.R.Jaiswal[2] and P.N.Godbole[3]

Ph.D. Scholar[1], Professor[2], Emeritus Professor[3]
Department of Applied Mechanics
Visvesvaraya National Institute of Technology, Nagpur 440011, India.

ABSTRACT

Tall reinforced concrete (RC) chimneys are wind sensitive structures and they exhibit both along-wind and across-wind response. The design is governed by combined response of along- and across-wind directions. The combination of along- and across-wind response is discussed in the first part of this paper. Combination approach followed by IS 4998:1992, ACI 307:1998 and Menon and Rao (1997b) have been discussed. Similarities and differences in these combination approaches are identified by evaluating the combined wind response for a RC chimney. In the second part, this paper explores the possibility of using existing maintenance platforms as tuned mass dampers (TMD) to control the combined wind response of RC chimney. With the help of a two-flue RC chimney of 217m height, it is shown that maintenance platform can indeed be used as TMD. These platforms are to be mounted on bearings which imparts the required lateral stiffness. It is shown that the maintenance platforms as TMD can reduce the combined response by about 30%.

Key words : chimney, tuned mass damper, maintenance platforms, along and acoss wind response.

INTRODUCTION

Chimneys are used to discharge pollutants at higher elevations. Tall reinforced concrete (RC) chimneys are sensitive to wind vibrations under the influence of dynamic wind loads. They oscillate in along- and across-wind directions. Along-wind vibrations occur due to gust in the direction of the incident wind and are associated with drag forces. Across-wind vibrations occur due to vortex shedding, leading to development of lift forces in the direction normal to the flow of the incident wind.

Indian code IS 4998:1992 specifies the methods for obtaining along- and across wind loads on tall RC chimneys. In this code, simplified and random response methods are given. Further, this code mentions that the design wind loads are to be obtained by combining the across wind response with the coexisting along wind loads. The combination of across- and along-wind loads is an issue, which needs to be properly discussed and interpreted. In this context, it is to be noted that the ACI 307:1998 and Menon and Rao (1997b) have also given similar approaches for combining the across-wind response with the coexisting along-wind response. In the first part of this paper, the issue of combination of along- and across-wind response as given in IS 4998:1992, ACI 307:1998, and Menon and Rao (1997b) is discussed. In the second part of the paper, the control of combined wind response using tuned mass damper(TMD) is studied. In the earlier study by Fulzele et al (2009), pendulum type TMD for controlling the wind response of RC chimney has been discussed. Detailed study on this topic has been performed by Jaiswal and Srinivas (2005), Srinivas (2005), Brahme (2008), Areemit and Warnitchai (2001) and Gerges and Vickery (2003). In these studies, pendulum type TMD has been shown to be effective in reducing the across-wind and along-wind response. It is noted that in many of the recent studies on TMD, the approach has been to use the existing component

of the structure as TMD (Makino et.al (2008), Chey et al (2008) and Johnson et al (2003)). In tall RC chimneys with multiflue, maintenance platforms are deployed at regular intervals along the height to support fire-brick linings. Fulzele et al (2009) have made an attempt to use one of the maintenance platform as TMD. In the present study, the work of Fulzele et al (2009) is extended further to study the effect of TMD on the along-wind, across-wind and combined response.

ALONG AND ACROSS WIND ANALYSIS

The along-wind analysis is performed using the random response method of IS 4998:1992. This method is suitably modified as per Manohar (1972) to use the actual mode shapes obtained from the dynamic analysis.The across-wind analysis is done as per Vickery-Basu method (1983, 1984). The wind climate parameters considered are the same as those used by Jaiswal and Srinivas (2005) and Fulzele at al (2009). The along-wind analysis is performed using the first three modes. For the across-wind analysis, modes whose critical velocity is less than the design wind velocity are considered.

The geometric details of a RC chimney considered for analysis are given in Figure 1. Height of the chimney is 217 m, which has five tapers. M30 grade concrete is used upto 138 m height and M25 grade is used in the remaining top portion. The mass density of concrete is taken as 2.5 t/m3, Young's modulus of the concrete is taken as 5000?fck , where fck is characteristic strength of the concrete and the structural damping as a fraction of critical damping is considered as 0.016. This chimney has twenty-one platforms along its height. Weight of each platform and the height at which platforms are located is given in Table 1. Each platform consists of circular RC slab of 200mm thickness supported on steel girders which rests on RC shell. A typical sketch of platform details is given in Figure 2. Total weight of all the platforms is 43,500 kN and the weight of RC shell is 1,40,000 kN.

For the purpose of analysis, the chimney is modeled as a vertical cantilever fixed at the base having varying cross sections using beam element (NKTP 12) of NISA software (EMRC,1998). The chimney is divided into 217 finite elements along its height. Natural frequency and mode shapes are obtained by using the free vibration analysis of the finite element model.

The natural frequencies of the first three modes of the chimney are obtained as 0.33 Hz, 1.41 Hz, and 3.51 Hz. The mean design wind speed is 46.1 m/s. The critical wind velocities of first three modes are calculated as 24.7 m/s. 103.8 m/s, 258.5 m/s. Since the critical wind velocity of first mode is less than the mean design wind speed, across-wind analysis is performed with only first mode. It is found that the across-wind response is a maximum at the mean design wind speed of 26 m/s which is very close to critical wind speed of 24.7 m/s. The base moments due to along-and across-wind loads are given in Table 2. The along-wind response given in Table 2 represents the peak value. Chimney tip deflection corresponding to the across-wind oscillation is obtained as 0.123 m.

The along-wind response consists of mean and fluctuating components. For the purpose of combination of along- and across-wind response, the coexisting along-wind response is required at a wind velocity at which the across-wind response is maximum. The along-wind response at this velocity is also given in Table 2.

Table 1: Platform details of the chimney

Platform no.	Height (m)	Platform weight (kN)
21	217	549
20	208	1809
19	198	1960
18	188	1977
17	178	1994
16	168	2011
15	158	2028
14	148	2046
13	138	2063
12	128	2081
11	118	2099
10	108	2117
9	98	2157
8	88	2198
7	78	2240
6	68	2283
5	58	2327
4	48	2418
3	38	2513
2	28	2611
1	23	1986

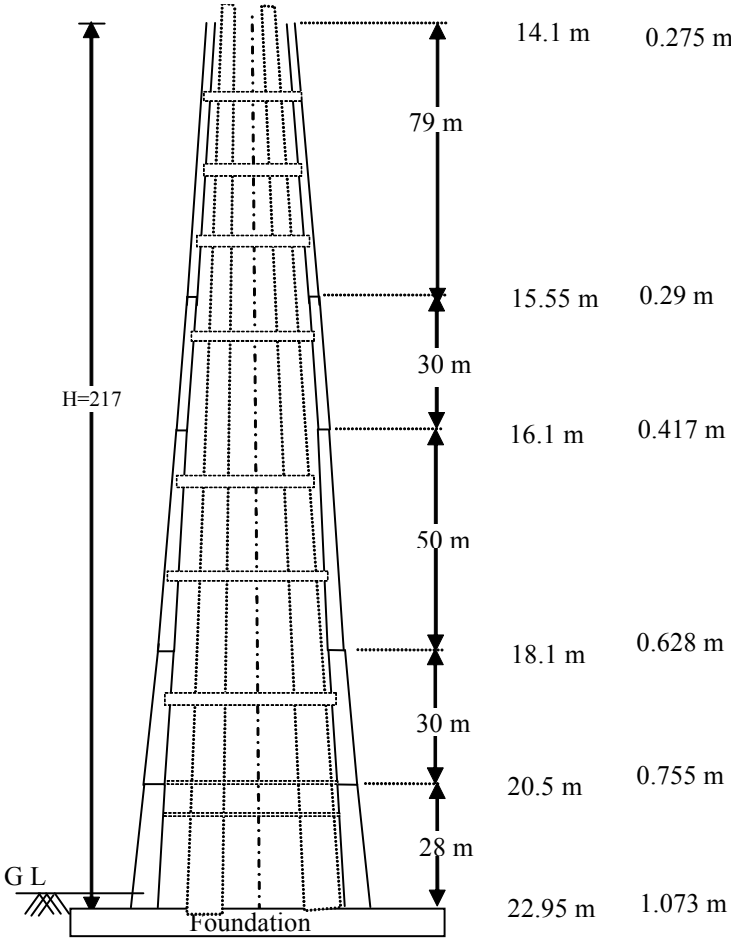

Figure 1: Details of 217 m high two-flue chimney

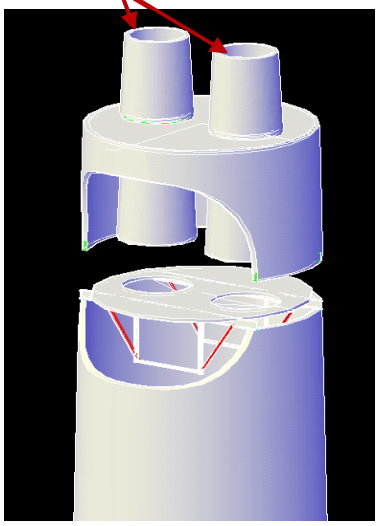

Sectional view of chimney showing the maintenance platform

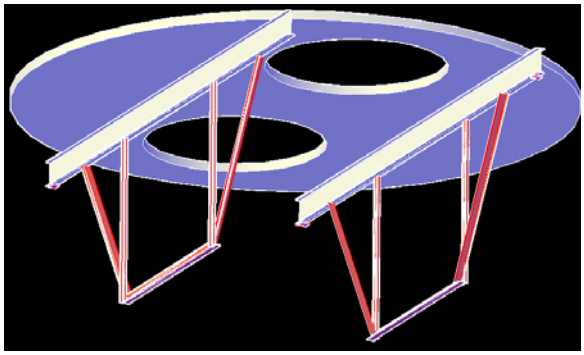

3-D view of steel girders supporting the RC slab of platform

Figure 2: Geometric details of maintenance platform

Table 2: Results of along and across-wind analysis

Response	Base moment (kNm)
a. **Along-wind analysis** (as per IS 4998:1992)	
i.Total response	662526
Mean component	351365
Fluctuating component	311161
ii.Coexisting total response	199337
Mean component	105717
Fluctuating component	93620
b. **Along-wind analysis** (as per Menon and Rao (1997a))	
i.Total response	788763
Mean component	351365
Fluctuating component	437398
ii.Coexisting total response	237319
Mean component	105717
Fluctuating component	131602
c.**Along-wind load with reduced mean component** (as per ACI 307:1998)	326080
Across-wind analysis	349130

COMBINATION OF ALONG - AND ACROSS-WIND RESPONSE

As mentioned earlier, chimney is designed for combined response of along- and across-wind loads. Codes follow different approaches for combining the along- and across-wind response. Here, the combination approaches used in IS 4998:1992, ACI 307:1998 and Menon and Rao(1997b) are discussed. The combination of along- and across wind response aquires significance due to the fact that the probability of peak response of along- and across-wind occurring significantly is much smaller than the probability of each occurring separately. To account for this, different approaches are used for combination.

IS 4998:1992 (Method-1):

In IS 4998:1992 the combined design moment at any section is taken as the square root of sum of squares of the moments due to the across-wind loads and the co-existing along wind loads. This implies that along-wind loads are to be calculated at the wind speed at which the across-wind loads are maximum. In the present study, across-wind reponse is maximum at a wind velocity of 26 m/s. The along-wind moments at the design wind speed of 26 m/s is 199337 kNm . Then, the combined base moment is obtained as

$((199337)^2 + (349130)^2)^{1/2} = 402028$ kNm.

ACI 307:1998 (Method-2)

In ACI 307:1998 the combined design moment Mw (z), at any section is taken as

$$M_w(z) = \left\{(M_a(z))^2 + (M_l(z))^2\right\}^{0.5} \quad (1)$$

where $M_a(z)$ = Moment induced by across-wind loads, $M_l(z)$ = moment induced by the mean along wind loads ($w_l(z)$)

where, $w_1(z) = \overline{w}(z)\left[\frac{\overline{V}}{\overline{V}(z_{cr})}\right]^2 \leq \overline{w}(z)$ (2)

$\overline{w}(z)$ = mean load per unit length, $\overline{V}(z_{cr})$ is mean wind speed at z_{cr} (i.e., 5/6 th of height) and $\overline{V}$ is evaluated between $0.5\,\overline{V}(z_{cr})$ and $1.3\,\overline{V}(z_{cr})$. The mean load, is calculated as per IS 4998 (1992). The value of Ml(z) is obtained as 326080 kNm. The combined design base moment is obtained as $((349130)^2 + (326080)^2)^{1/2} = 477723$ kNm. It is intriguing to note that as per ACI 307:1998, the mean component of along-wind response is reduced by a factor of $(\bar{V}/\bar{V}(z_{cr}))^2$, which does not depend on the critical wind velocity at which the across-wind response is maximum.

Menon and Rao (1997b) (Method-3)

The along-wind response obtained by Menon and Rao(1997a) uses an effective gust factor(Gz) which varies along the height is given by

$$G_z = G_0\left[1 + \left(\frac{1.55 - 0.0005h}{6}\right)\left(\frac{z}{h}\right)\right] \quad (3)$$

The dynamic along-wind load at a velocity at which across-wind response is maximum is given by $w_{dz} = (3(G_z\text{-}1)\ z\ M_m0)/h^3$, where M_{m0} is moment at base due to mean wind load. The mean wind load is calculated as per IS 4998 (1992). G_0 is the gust factor at the base of the chimney (i.e., z = 0), G_z is the effective gust factor at height z. The across-wind moment needs to be combined with coexisting along-wind moment to obtain the resultant maximum moment under the across-wind loading condition. The combined design moment is given by,

$$M_z = M_{zac,r}\sqrt{1 + \left[(M_{zac,r}/M_{dz})^2 - (G_z - 1)^2\right]^{-1}} \quad (4)$$

Where $M_{zac,r}$= across-wind moment at height z in rth mode, M_{dz} = coexisting along-wind moment due to dynamic wind load. The values of G_0, G_z and w_{dz} are calculated as per the procedure given by Menon and Rao(1997a). Then, the base moment due to dynamic wind load is calculated as 131602 kNm, and the acoss-wind load is obtained as 349130 kNm. From equation 4, the combined design moment is obtained as 383021 kNm.

Table 3: Combination of along and across-wind response

Sr no	Method	Base moment (kNm)		
		Along	Across	Combined
1	Method-1	199337	349130	402028
2	Method-2	326080	349130	477723
3	Method-3	131602	349130	383021

The results obtained from the three methods are given in Table 3. The across-wind moment used in all the three methods is the same and is obtained by Vickery-Basu (1984) method. It is reiterated that, for all the three methods, the along-wind loads were obtained using IS 4998:1992, but the combination was done as per the procedures mentioned in the above methods.

From Table 3, it is seen that, in IS 4998:1992 the total along-wind response at the coexisting velocity is combined with across-wind response. In ACI 307:1998, the mean component of along-wind response is

multiplied by a factor $(\overline{V}/\overline{V}(z_{cr}))^2$ and then it is combined with across-wind response. In the method suggested by Menon and Rao (1997b) the fluctuating component of mean load evaluated at the coexisting velocity is combined with the across-wind moment. It is seen that the combined moment obtained from IS 4998:1992 matches reasonably well with the value obtained by Menon and Rao(1997b).

MAINTENANCE PLATFORMS AS TMD

As mentioned earlier, in the past many studies (Jaiswal and Srinivas (2005), Brahme (2008), Areemit and Warnitchai (2001) and Gerges and Vickery (2003)) have shown that pendulum type TMD can be quite effective in reducing the wind response of tall chimneys, particularly the across-wind response. Further, Makino et.al (2008) ,Chey et al (2008) and Johnson et al (2003) have attempted to use the existing components of the structure as TMD. For tall RC chimneys, the maintenance platforms are provided at various heights. A typical platform consists of circular RC slab supported on steel girders which in turn rest on RC shell (Figure 2). If this platform mass is to be used as TMD, then it must have sufficient lateral stiffness to act like TMD. This lateral stiffness can be imparted by supporting the platform on bearing as shown in Figure 3b.

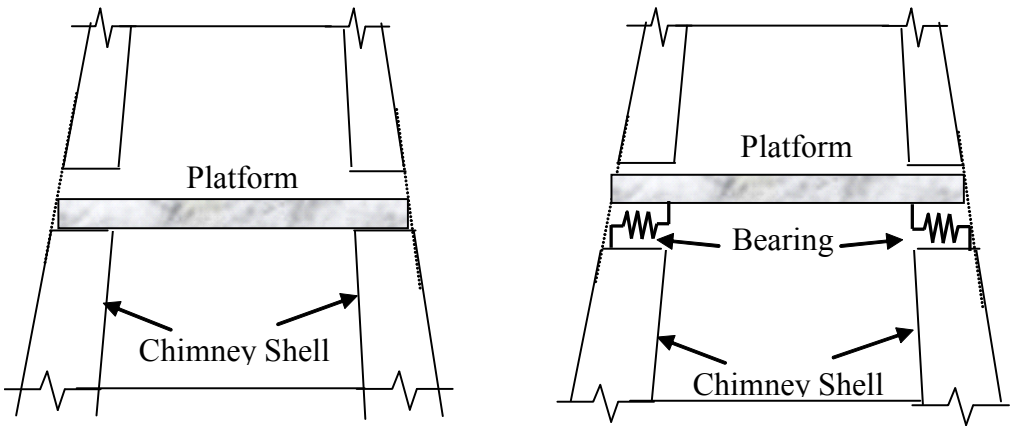

a. Existing case b. Proposed changes

Figure 3: Details of maintenance platform and elastomeric bearing as TMD

Recently, Fulzele et al (2009) have shown that for a 217 m tall RC chimney, one of the existing platform located at 208 m height, can be used as TMD if it is supported on suitable bearings. But in the analysis, the authors have not considered the weights of the platforms. In the present study, for the same chimney, the weight of all the platforms is considered in the analysis. The total weight of chimney analysed here is 1,83,500 kN, which includes the platforms weight of 43,500 kN. The weight of platform at a height of 208 m is 1808 kN, which is considered as TMD, is about 1 % of the total weight (Ricciardelli (2001)). The generalized mass, which is a sum of the product of the mass per unit height and the corresponding modal value, is calculated as 2311 t. Hence, the ratio(μ) of the TMD mass to that of generalised mass is 0.0782. Since the frequency of the first mode of chimney(f1) is 0.33 Hz, the frequency of the TMD, $f_t = f_1/(1+\mu) =$

0.31 Hz. Then, the stiffness of the TMD spring is obtained as, $k_t = 4 \pi_2 f_t^2 m_t = 694.3$ t/m. Thus the bearing as shown in Figure 3b, which is proposed to be mounted at the bottom of the platform, shall have total stiffness of 6943 kN/m.

For the analysis, TMD is modeled as spring and mass attached to the beam element of chimney.Then, using the finite element model, the free vibration characteristics of the chimney with TMD have been obtained. The natural frequencies for the first three modes are obtained as 0.28 Hz, 0.37 Hz and 1.44 Hz respectively. It is noted that the critical wind velocity of the first two modes of chimney with TMD are found to be less than the mean design wind speed. Hence, the across-wind analysis is performed by considering the first two modes. The results of along and across-wind analysis for the chimney with and without TMD are presented in the Table 4 and 5.

It is to be noted that across-wind response is obtained as per Vickery and Basu (1983). The details of across-wind response in each mode are already given in Jaiswal and Srinivas (2005). For both the modes the model response is combined as per the square root of sum of squares rule. By using a similer approach Vickery and Basu (1984) have used the multiple modes to predict the the response of a tower. The structural damping ratio is taken as 0.016 for the analysis of chimney with and without TMD.

Effect of TMD on wind response

From Table 4 it is noted that TMD does not help in reducing the alongwind response, but it significantly reduces the across wind response. The reduction in the across-wind peak tip deflection, base shear and base moment are noted as 16.3%, 40.6% and 39.1% respectively. The deflection of TMD is obtained as 0.32 m as against the chimney peak tip deflection of 0.103 m. The higher deflection of TMD (i.e., maintenance platform) is quite on the expected lines and this deflection can be accommodated by the maintenance platform. Further by increasing the damping of the platform-spring system, this deflection can be reduced.

Table 4: Results of along-wind analysis

Chimney	Base shear (kN)	Base moment (kNm)
Without TMD	5079	662526
With TMD	5097	664299
% of reduction	-0.3%	-0.2 %

Table 5: Results of across-wind analysis

Chimney	Mean velocity V (m/s)	Tip deflection η (m)	Base shear (kN)	Base moment (kNm)
Without TMD	26	0.123	2245	349130
With TMD	30	0.103	1333	212722
% of reduction	-	16.3 %	40.6 %	39.1 %

The design of chimney is carried out for the combined response of along and across-wind analysis. The comparison of combined response with and without TMD is presented in Table 6 for all the three methods. For chimney with TMD, two modes are to be considered in the across wind analysis. Hence in the merthod by Menon and Rao (1997b), while using the equation (4), $M_{zac,r}$ is taken as total across wind response of the first two modes. It is observed that the combined design values have considerably reduced due to TMD in all the three methods.

Table 6: Combined design moments using maintenance platform as TMD

Sr. No.	Method	Chimney	Base moment (kNm)
1	Method-1 (IS 4998:1992)	Without TMD	402028
		WithTMD	295477
		% reduction	**26.5**
2	Method-2 (ACI-307:1998)	Without TMD	477723
		With TMD	389331
		% reduction	**18.5**
3	Method-3 (Menon and Rao 1997b)	Without TMD	383021
		With TMD	241619
		% reduction	**36.9**

5. DISCUSSION AND CONCLUSIONS

The design of tall RC chimney mainly depends on the combined values of along and across wind loads. In the present work, the approaches for combining the along and across wind response as followed by IS 4998:1992, ACI 307:1998 and Menon and Rao(1997b) are reviewed. It is noted that IS 4998:1992 combines across-wind response with the co-existing along-wind response, i.e., total along-wind response is obtained at a velocity at which across-wind is maximum. In ACI 307:1998 the along-wind response used for combination is calculated at reduced mean velocity component. This reduced mean velocity component does not depend on the critical wind speed. Menon and Rao (1997b) have used fluctuating component of alongwind response to combine with the across-wind response. The fluctuating component of along-wind response is obtained at a velocity at which acrosswind response is maximum. The combined response obtained by ACI 307:1998 is on higher side compared with IS 4998:1992 and Menon and Rao(1997b) .

In the past studies (Jaiswal and Srinivas (2005), Brahme (2008)) , Areemit and Warnitchai (2001) and Gerges and Vickery (2003)), it has been shown that, the pendulum type TMD can be used to control the wind response. Subsequently, Fulzele etal (2009) made an attempt to use the existing platform as pendulum type TMD. The present study performed on two-flue RC chimney of 217 m height, indicates that maintenance platform can indeed be used to control the combined wind response (i.e., combined response of along and across wind analysis).

For tall RC chimneys with multiflue, maintenance platforms are present at various heights. One of these platforms at higher elevation, can be used as TMD by providing it with suitable lateral stiffness.Analysis of a two-flue RC chimney of 217 m height indicates that platform indeed have appropriate mass to act as TMD and lateral stiffness can be imparted by providing suitable elastomeric bearings at the support. Such a TMD reduces the combined response by 20-30%. The deflection of platform is 0.32 m, which can be permitted without affecting the functional requirements of maintenance platforms.

The results obtained in this study shows that the maintenance platforms offer a good option to be used as TMD to control the combined wind response of tall chimneys. The maintenance platform is to be mounted on lateral springs (like eastomeric bearings) to impart lateral stiffness. Further studies on wind tunnel model are neccessory to validate the results of this study.

ACKNOWLEDGEMENTS

This work is part of a R&D project funded by the University Grants Commission, Government of India, New Delhi.

REFERENCES

1. ACI 307 (1998). "Standard practice for design and construction of RC chimneys(ACI 307-98) and commentary(ACI 307R-98)',American Concrete Institute, Detroit.
2. Areemit, N. and Warnitchai, P. 2001. "Vibration suppression of 90m tall steel stack by using a high damping tuned mass damper", 8th East Asia-Pacific Conference on Structural Engineering & Construction, Nanyang Technical University, Singapore.
3. Bramhe, H.S. (2008). "Analysis of tall structures for dynamic wind loading", M.Tech. thesis, Department of Applied Mechanics, VNIT, Nagpur, India.
4. Chey, M.H., Carr, A.J., Chase, J.G. and Mander, J.B. (2008). "Resetable tuned mass damper and its application to isolated stories building system." 14th World Conference of Earthquake Engineering, Paper No. S25-018, Beijing, China.
5. EMRC (1998), "User's Manual for NISA II: Numerically Integrated Elements for for System Analysis", Engineering Mechanics Research Corporation, Michigan, USA.
6. Fulzele, V., Reddy, K.R.C. and Jaiswal, O.R. (2009). " Use of maintenance platforms as TMD in tall RC chimneys", Proc. Of 5th National Conf. Wind Engg., SVNIT,Surat, India, 247-256.
7. Gerges, R.R. and Vickery, B.J. (2003). "Wind tunnel study of the across-wind response of a slender tower with a nonlinear tuned mass damper", J. of Wind Eng. & Ind. Aerodyn, 91, 1069-1092.
8. IS 4998 (part-1). (1992). "Criteria for design of reinforced concrete chimneys", Bureau of Indian Standards, New Delhi.
9. Jaiswal, O.R. and Srinivas, V. (2005). "Effect of tuned mass damper on across-wind response of tall RC Chimneys", J.of Wind and Engineering, India, Vol. 2, No.1, 9-21.
10. Johnson, J.G., Reaveley, L.D. and Pantelides, C. (2003). "A rooftop tuned mass damper frames", Earth quake Engineering and Structural Dynamics, 32, 965-984.
11. Makino, A., Imamiya, J. and Sahashi, N. (2008). "Seismic vibration control of a high-rise RC buildings by a large tuned mass damper utilizing whole weight of the top floor.", 14th World Conference of Earth quake Engineering, Paper No. S05-02-003, Beijing, China.
12. Manohar, S.N. (1972). "Design and Construction of Tall Chimneys", McGraw-Hill Book Co., New York.
13. Menon,D. and Srinivas Rao, P. (1997a). "Estimation of along-wind moments in RC chimneys", J. of Engineering Structures, Vol.19, No.1, 71-78.
14. Menon,D. and Srinivas Rao, P. (1997b). "Uncertainities in codal recommendations for across-wind loads analysis of RC chimneys", J. of Wind Engg. & Ind. Aero., 72, 455-468.
15. Ricciardelli, F. (2001). "On the amount of mass to be added for the reduction of the shedding induced response of chimneys", J. of Wind Eng. & Ind. Aero., 89, 1539-1551.
16. Srinivas, V. (2005). "Use of TMD to control wind response of tall chimneys", M.Tech. thesis, Department of Applied Mechanics, VNIT, Nagpur, India.
17. Vickery B.J. and Basu R.I. (1983). "Across-wind vibrations of structures of circular cross-section. Part-I. Development of a mathematical model for two-dimensional conditions", J. of Wind Eng. & Ind. Aero., 12, 49-73.
18. Vickery B.J., Basu R.I. (1984), "The response of reinforced concrete chimneys to vortex shedding", J. of Engineering Structures, Vol. 6, 324-333.

Journal of Wind and Engineering, Vol. 8, No. 1, January 2011, PP. 10-22

FLOW SIMULATION OF LOW - RISE BUILDING MODELS IN A WIND TUNNEL AND COMPARISION WITH FULL SCALE DATA

K. Narayan*, A. Gairola**

*Associate Professor, Deptt of Civil Engg. I.E.T. Lucknow, India
**Associate Professor, Deptt. of Civil Engg. I.I.T. Roorkee, India

ABSTRACT

This paper presents the flow simulation and pressure measurements in a boundary layer wind tunnel for a Wind Engineering Research Field Laboratory, Texas Tech University building model of 1:25 scale and comparison with full scale field data. The full-scale and model scale values of mean pressure, Cpmean, are mostly consistent for similar wind directions whereas the rms and peak values show rather larger deviations for certain wind directions.

Keywords: flow simulation, TTU building, low -rise building.

INTRODUCTION

Wind tunnel predictions of surface pressures and wind loads are considered to be successful only if the flow in the atmospheric boundary layer is simulated properly. Such simulations entail development of boundary layers in long test-section wind tunnels over simulated upwind terrain roughness. With this approach, model scales of the order of 1:500 are needed, but these are rather small for low-rise structures. In order to overcome this problem, wind loads on low-rise buildings at scales of 1:25 to 1:100 are currently obtained in turbulent flows which simulate only the lower region of the atmospheric boundary layer or atmospheric surface layer. Two approaches to this simulation problem were developed. The first approach emphasized that the velocity profile and the turbulence integral scale are the pertinent simulation criteria (Cook, N.J. (1978). Duplication of the mean-velocity profile was considered to be attained either with equality of the Jensen Number or by duplication of the power-law exponent. The second approach concentrated primarily on the duplication of the turbulence intensity profile. Specifically, duplication of this intensity at roof height was recommended, while the turbulence integral scale should be at least as large as the largest model dimension (Tieleman, 1978). No consensus was reached on which simulation approach provided the best results. Full /model scale-comparison of the mean and fluctuating pressure coefficients showed generally good agreement, except in critical surface areas where extreme suctions dominate, the latter observed primarily in regions of flow separation and vortex development.

Mehta et al (1992) have presented roof corner pressure data collected on the Wind Engineering Research Field Laboratory Building hereinafter called the TTU building. . It has been found that Cp mean values are consistent for different records with similar angle of wind attack while Cpmin show scatter and its value touches -12.0. This occurred at angle of wind attack between 180° and 270° where conical vortices form on the roof above the instrumented corner. It is also found that very large negative peak pressure coefficients are obtained for long periods of time. Results obtained by full-scale studies are compared with the wind tunnel results. Comparison of full-scale/model-scale results gave new directions for flow

simulation and for pressure measurement techniques for testing the models of low buildings in the wind tunnel. With the availability of full-scale data for low buildings, the techniques for wind flow simulation have to be reviewed on the basis of model/full-scale comparison of observed surface pressures. Jamieson and Carpenter (1993) conducted wind tunnel pressure measurement on 1:25 scale-model of the Texas Tech Building. Comparison with full-scale data for Mode M04 shows generally good agreement for mean, rms, and peak data for wind directions producing peak suction. However, some differences were observed in the rms and peak data, particularly for wind directions not showing large peak pressures. Additional pressure taps located closer to the roof edges than any of the full-scale taps produced very large suction, with a peak pressure coefficient which could be as high as around -15.

A good flow simulation based on duplication of the mean-wind profile, the along-wind turbulence intensity and integral scale, does not automatically guarantee duplication of peak suctions from the field experiments (Tieleman 1996). Instead, exploratory experiments which stress the duplication of both horizontal turbulence intensities and their small-scale turbulence content are able to duplicate these extreme suction pressures much better (Tieleman 1996). Cheung et al (1997) carried out a study on wind pressures on a 1/10 scale model of the TTU building and concluded that the mean and rms pressure coefficients from the model for critical corner tapings for oblique wind directions are in excellent agreement with the corresponding full-scale values. The largest minimum peak pressure coefficients for these tappings are approximately 20% less in magnitude than the corresponding full-scale values.

Tieleman et al (1998) conducted experiments on the roof of a 1:50 scale model placed in turbulent shear layers developed over several different roughness configurations in the boundary - layer wind tunnel which is part of the wind load test facility at Clemson University and compared with full scale data of pressure coefficients from the T.T.U. building. He concluded that agreement between model and field roof pressures is only possible provided detailed attention is paid to the duplication of the two horizontal turbulence intensities and their small-scale turbulence content, and the model turbulence integral scale exceeds one-fifth the magnitude of the scaled-down field scale. The results also show that the mean flow profile parameter α and z_0 do not require exact duplication.

Tieleman (1996) found that for Atmospheric Surface Layer (ASL) simulation, other than duplication of turbulence intensity, the small-scale spectral density parameter, S, of the incident flow, which is defined below, should also be properly matched. 'S' is given as,

$$S = (n\, S_u(n) / S_u^2)\, (S_u / U)^2 \times 10^6$$

evaluated at $n = 10U/L$

where,

n - Frequency of velocity fluctuations
Su - Standard deviation of the stream-wise velocity fluctuations
U - Mean velocity evaluated at building eave height, H
L - Characteristic model dimension, which is eaves height in the present study
Su (n) - Spectral density function at frequency n

Improved matching of the small-scale turbulence parameter can be achieved by using larger models together with increased upstream floor roughness or by using small spires in the upstream. Using larger models and increased floor roughness while relaxing the requirement for strict matching of integral scale has

produced flow simulation which provides a more acceptable laboratory duplication of the peak pressure coefficients in the critical areas (Tieleman et al 1998).

On the basis of the work reviewed it has been established that for the wind tunnel studies on low-rise buildings, the atmospheric surface layer (ASL) should be modeled. Proper simulation of turbulence intensities and small-scale turbulence content in the incident flow are required. Furthermore, exact scaling of the turbulence integral length scale does not seem essential for the prediction of the wind pressures on low-rise buildings.

TEST PROGRAMME

Boundary layer Wind Tunnel

The study has been conducted in the Boundary Layer Wind Tunnel (BLWT) at Indian Institute of Technology Roorkee, India. This is an open circuit, continuous flow, suction type wind tunnel using a single blower fan (125 HP) having a test section of 2.1m x 2.0m size. The length of test section is 15m. An elliptical effuser profile with contraction ratio 9.5:1 along with square-holed honeycomb at the entrance (6mx6m) helps to develop a uniform smooth flow in the test section (Fig 1). Different roughness devices have been used to meet the wind tunnel simulation requirements and for the development of highly turbulent flow for generating the Atmospheric Surface Layer in the 2.1m x 2.0m BLWT. Five Counihan type vortex generators, a barrier wall and roughness blocks of 15.0cm, 10.0cm and 7.0cm have been used as roughness devices. Layout of different roughness devices used for flow simulation is shown in Fig 2.

Photo 1 TTU Building Model with Flow simulation Roughness Devices

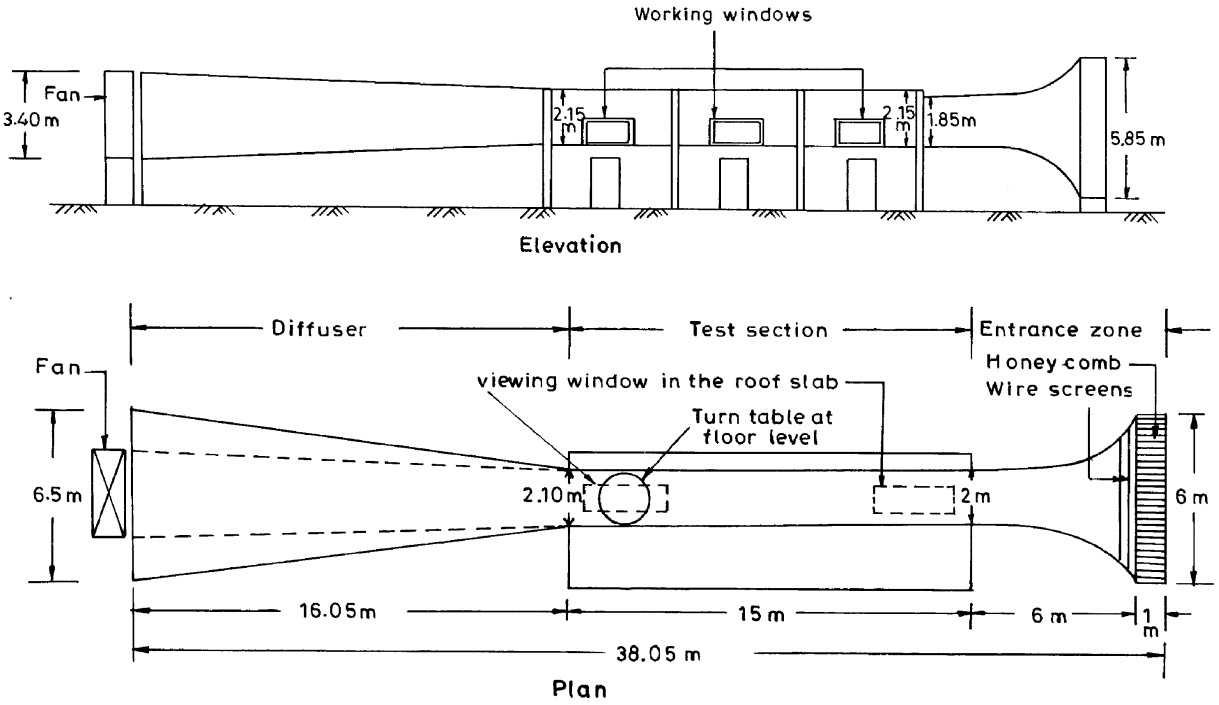

Fig 1 Schematic of Boundary Layer Wind Tunnel at Department of Civil Engineering, Indian Institute of Technology Roorkee, Roorkee, India

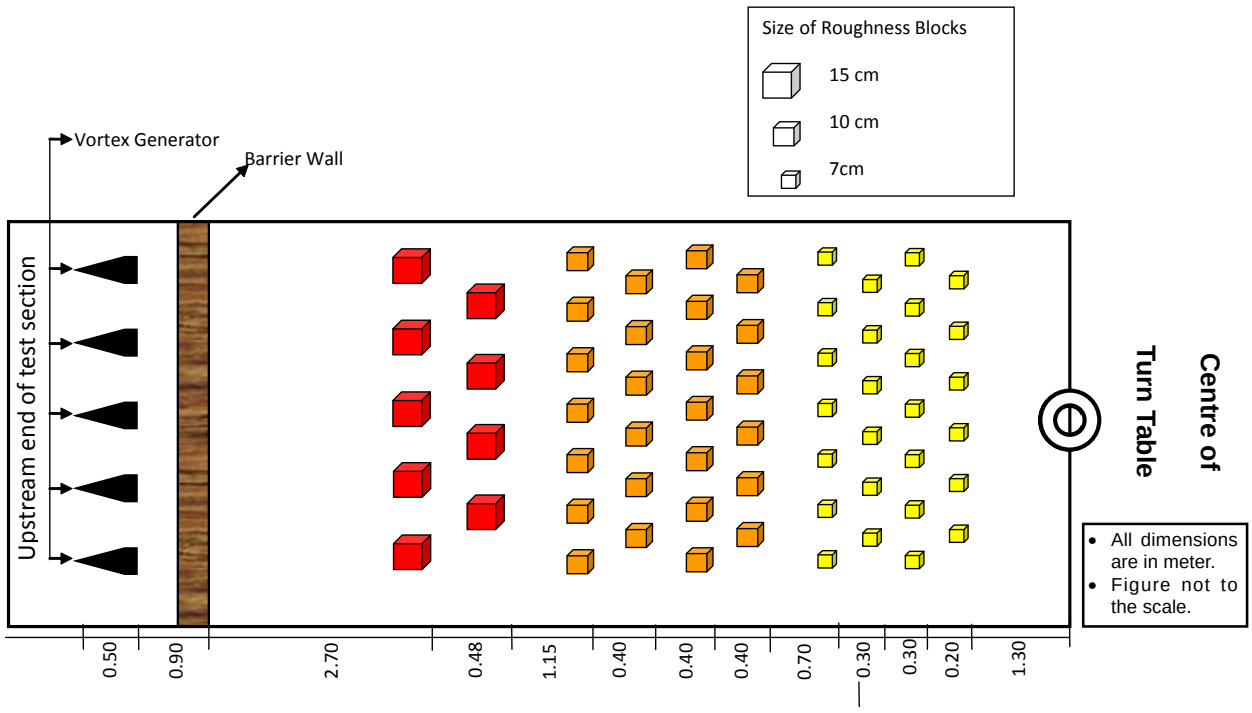

Fig. 2 Layout of Different Roughness Devices Use for Flow Simulation

Modelling of tubing system

Surface pressures on the roof of the building models have been measured by connecting steel taps of 1.0 mm internal diameter, which are flushed to model surface, to vinyl tubing of 1.2 mm internal diameter. A three stage tubing system is used for pressure measurement. Total length of tubing system used was 250 mm in length. A restrictor of 60 mm in length and 0.4 mm in diameter was connected at 150 mm from the pressure tap. Restrictor was connected to Scanivalve Pressure Scanner with 40 mm long 1.2 mm internal diameter vinyl tube. Amplitude frequency response of the tubing system was approximately flat and phase characteristic was linear upto a frequency of 200 Hz.

Establishing Flow Conditions

For flow measurements with the hot-wire system, a sampling frequency beyond 1 KHz and a 4-second length of record was adopted as a minimum requirement (Gupta1996). In the present study, instantaneous velocity fluctuations have been recorded using a single hot-wire probe at a sampling frequency of 4 KHz for a duration of approximately 4 seconds, viz, a total of 16384 samples are recorded at each point for flow characteristic measurements. The values of mean velocity and longitudinal turbulence intensity at the eaves height of the building model have been found to be 9.68 m/s and 20% respectively. The mean velocity and longitudinal turbulence intensity variations obtained in the wind tunnel are presented in Fig 3. The theoretical velocity profile variation (solid line), corresponding to $\alpha = 0.176$, is in the good agreement with the measured values.

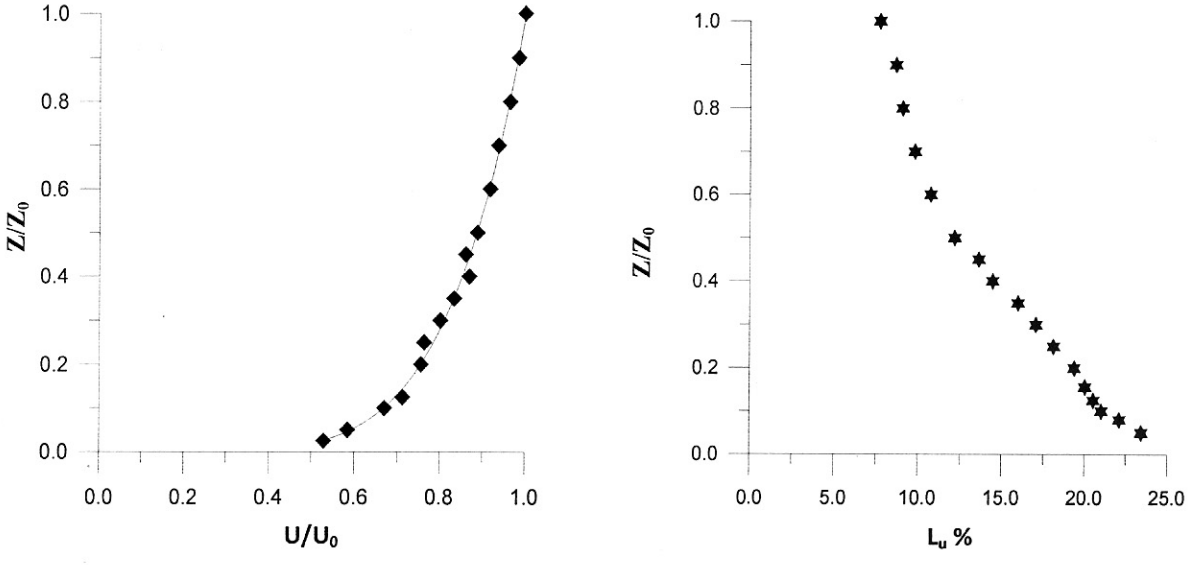

Fig 3 Mean Velocity and Turbulence Intensity Profiles for the Simulated Flow in Wind Tunnel

Auto correlations of the velocity fluctuations are calculated using Eq.1

$$R(\tau) = \lim_{T\to\infty} \frac{1}{T} \int_0^T v(t) \times v(t+\tau) dt \qquad (1)$$

where ν (t) is velocity fluctuation at time t and ν (t+τ) is velocity fluctuation after the small time increment of τ.

Fig.4 presents the auto-correlation plot of velocity fluctuations, recorded at eaves height of the model, i.e., at 15.6 cm from the tunnel floor. Auto-correlations are then used to evaluate the integral scale of turbulence. The integral scale is defined as the area under the auto-correlation curve of the fluctuating velocity component. These are usually temporal measurements at a fixed point and Taylor's hypothesis can be used to convert the area under the auto- correlation function into units of length as given by Eq.2.

$$L_{ux} = U\int_0^1 R(\tau)d\tau \qquad (2)$$

where L_{ux} is the integral length scale, U is the mean wind velocity and $\int_0^1 R(\tau)d\tau$ is the area under the auto-correlation curve [Scruton, 1981].

An average of ten observed values is taken as representative for L_{ux}, which is found to be 0.45m.

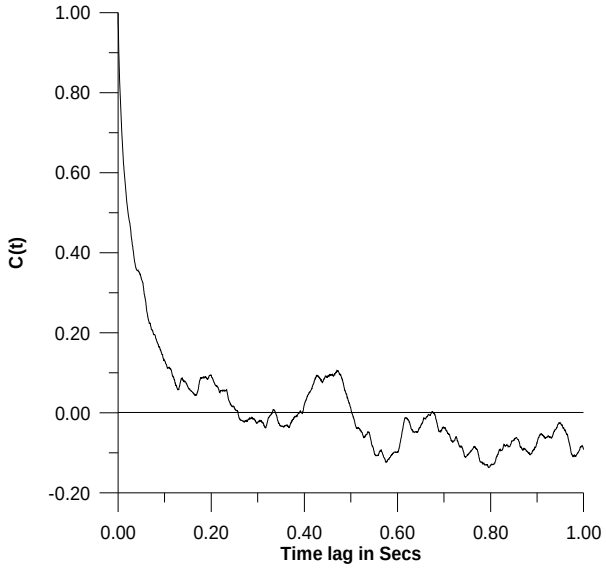

Fig 4 Auto Correlation Plot at Eave Height

The small-scale turbulence parameter of the incident flow is evaluated at the frequency n (=10U/ L) at model eave height. The average value of the small-scale parameter obtained was S = 101 which is quite high and found to be appropriate for the model study. Wind tunnel studies so far have been made with smaller values of S excepting one reported by Tieleman. The flow characteristics obtained with the present set of roughness devices closely agreed with the simulation # 8 of Tieleman et al (1999), which gave the best duplication of mean and peak pressure coefficients comparing model/full-scale results establishing adequacy of the 'S' value achieved. Tieleman et al (1997, 1998) earlier presented the value of the small scale turbulence parameter for different simulations but later corrected them in Tieleman et al (1999).

$n' = nH / U$ $S'(n) = nS(n) / \sigma 2$

Plots of n′ versus S′ (n) on log-log scale have been presented in Fig 5.

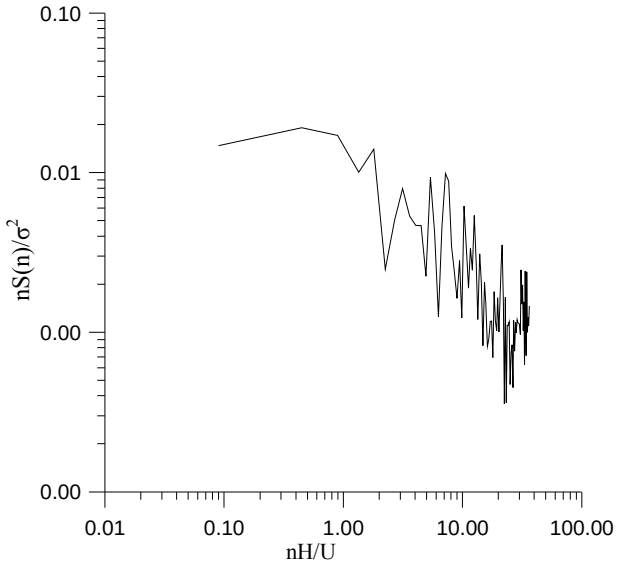

Fig 5 Normalised Reduced Spectrum Plot at Eave height

COMPARISON OF TTU BUILDING MODEL WITH FULL SCALE DATA

The TTU Building model was made in Perspex to 1:25 scale. This is an approximately flat roofed building with full scale dimensions 9.14m × 13.72m in plan and 3.96m high. Texas Tech University field data Mode M04 compiled by Bob Iverson & Marc Levitan has been downloaded through Internet site www.ttu.edu.com. Mode M04 consists of data for 9 taps. The first 7 taps (50101 - 50909) are roof corner taps and the last 2 taps (22306 and 42206) are wall taps. Each record is of 15 minutes duration and all records are sampled at 10 Hz. The mean wind tunnel velocity at roof height of the building is 9.68 m/s and the turbulence intensity is 20% which is close to the mean full scale value of TTU Mode M04 data.

Since the sample record length, Tp for the field observation is 900 s, the model record length, Tm, depends on the corresponding velocity, Vm, attained in the wind tunnel. With Tm = Tp(Lm/Lp)(Vp/Vm) [Tieleman et al 1998] and model scale 1:25, an average record length required for the simulation is approximately 30s in duration. Pressure coefficients from model experiments have been based on the velocity at the scaled roof height, which is 15.6 cm, observed at the model location. Flow parameters describing the incident flow have been acquired at the same location. Measurements have been made for 360º in steps of 15º. The observed pressure coefficients Cpmean, Cpmin and Cprms have been plotted against the angle of wind incidence varying from 0º to 360º and compared with the full-scale data. Figs. 6(a) to 6(e) show the comparison of pressure coefficients between model-scale and full-scale measurements from which the following behaviour is noticed:

1. Overall, the model-scale pressure coefficients showed generally good agreement with the full-scale data for the corresponding pressure taps. The mean values, Cpmean, particularly agreed well.

2. The full-scale mean pressure values, Cpmean, are mostly consistent for similar wind directions whereas the rms and peak values show rather larger deviations for certain wind directions.

3. Model-scale rms values, Cprms, matched the full-scale data quite well for the wind directions giving large peak values, but are found to be generally somewhat higher than the prototype values.

4. The peak wind pressures, Cpmin, are somewhat higher in the model tests for some taps for wind directions 225° and 270°.

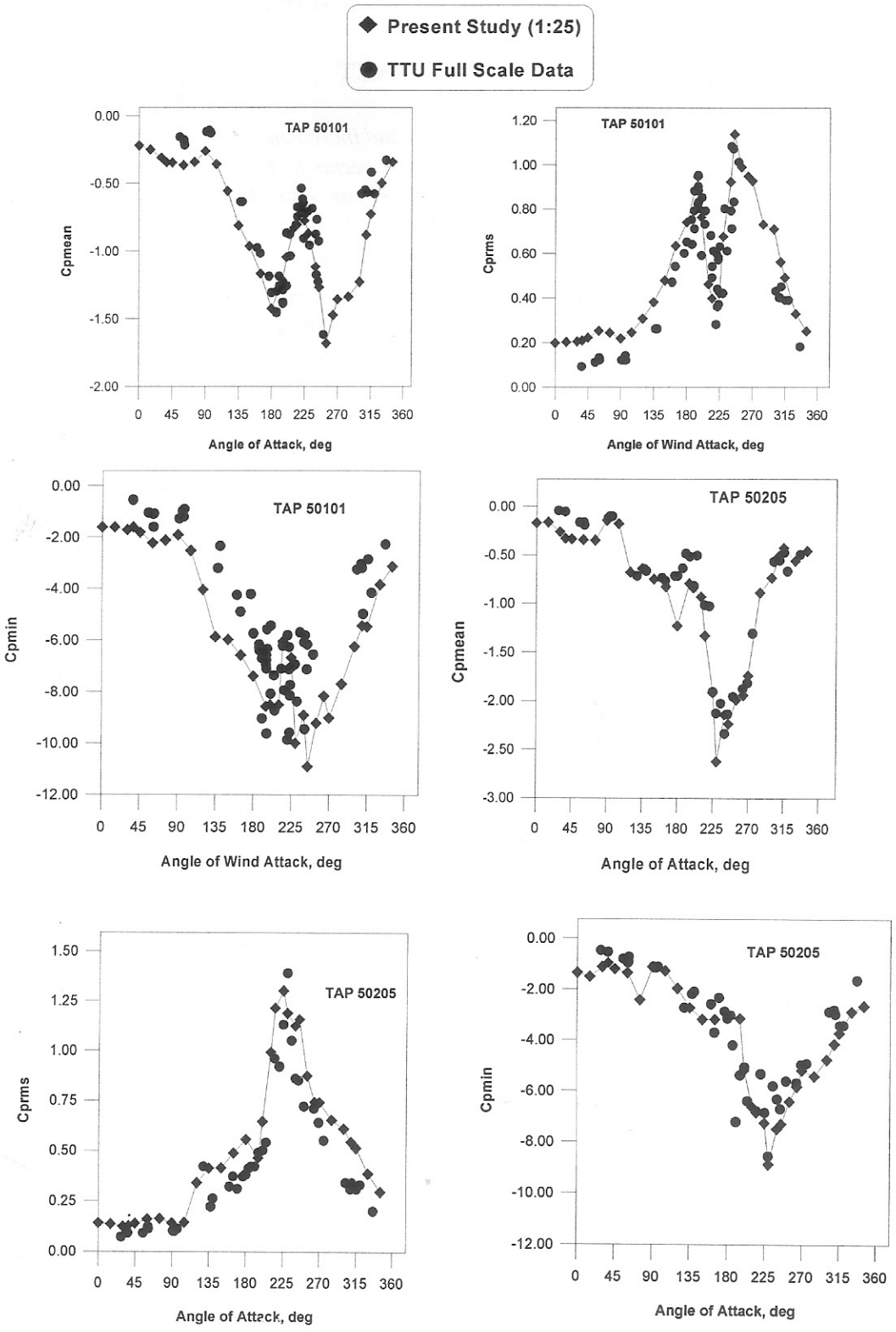

Fig 6 (a) TTU Building Cpmean, Cprms and Cpmin for Roof taps

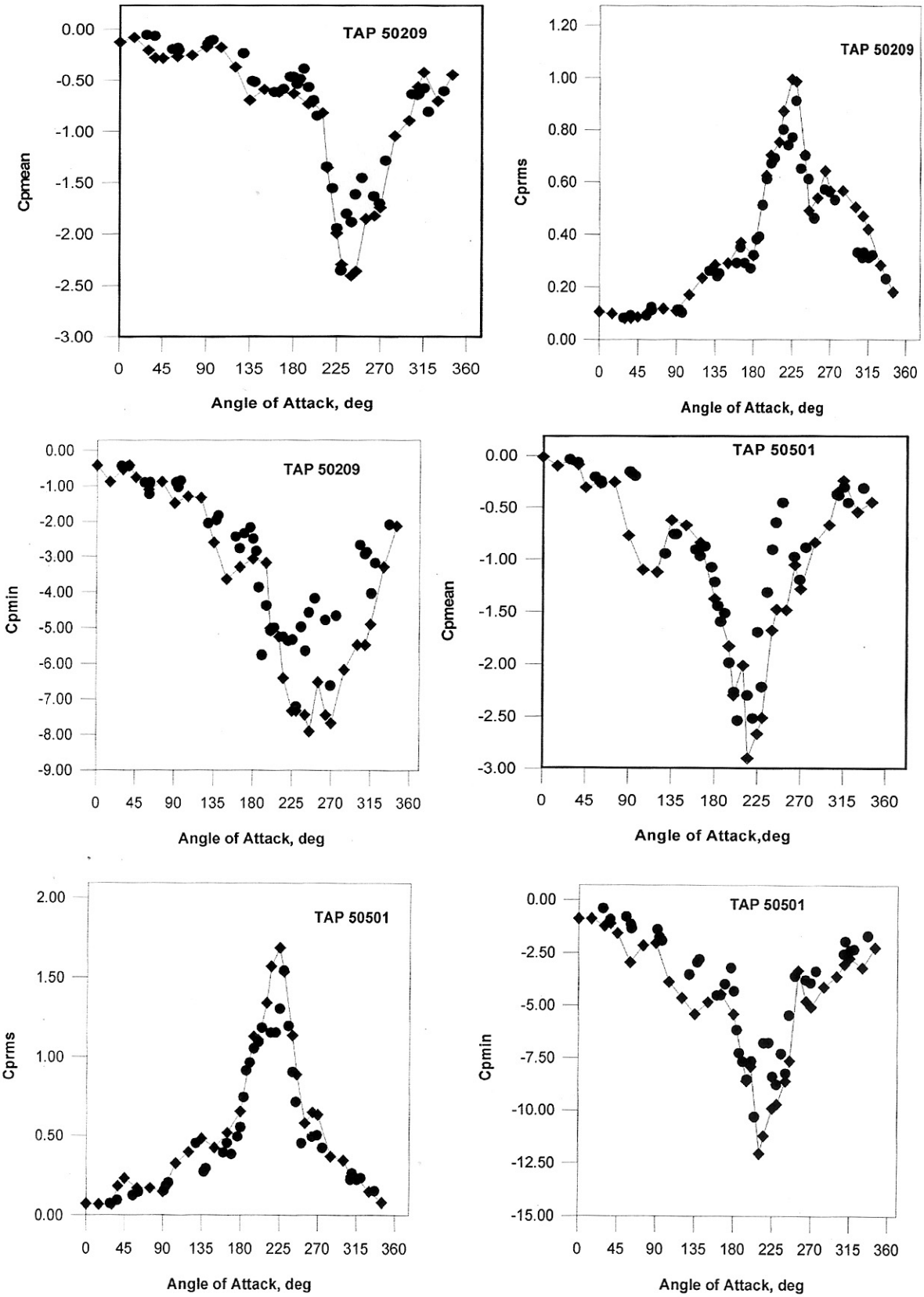

Fig 6 (b) TTU Building Cpmean, Cprms and Cpmin for Roof taps

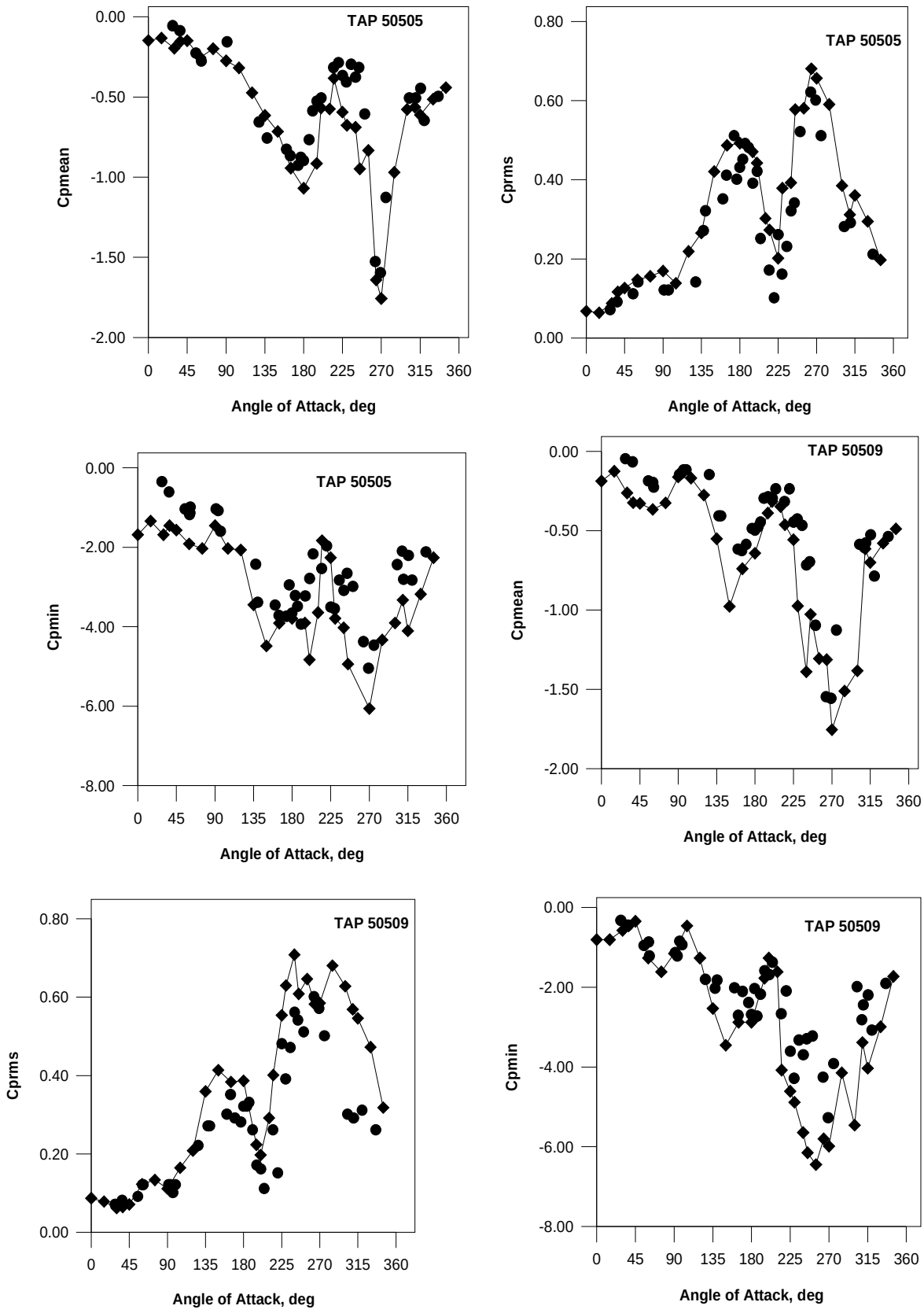

Fig 6 (c) TTU Building Cpmean, Cprms and Cpmin for Roof taps

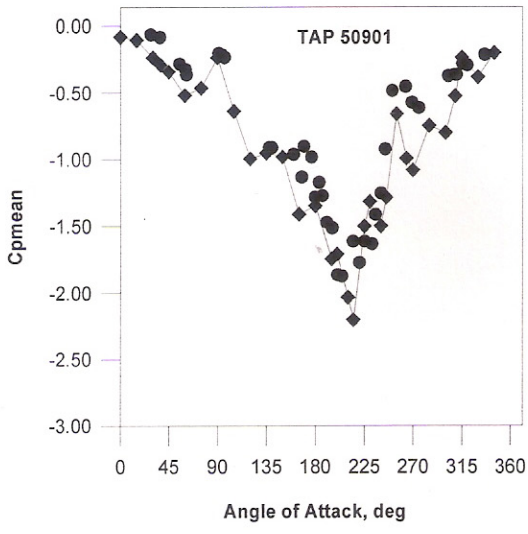

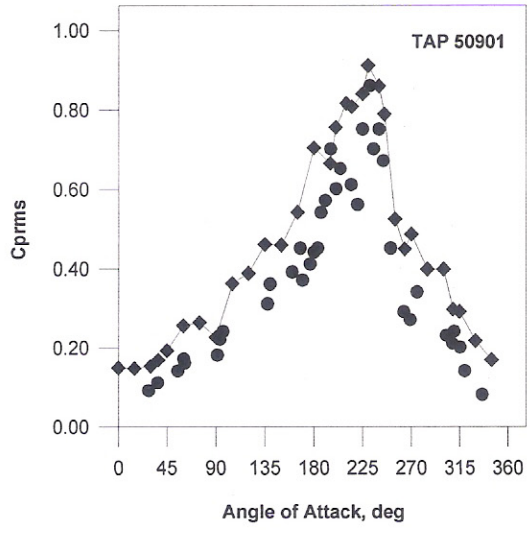

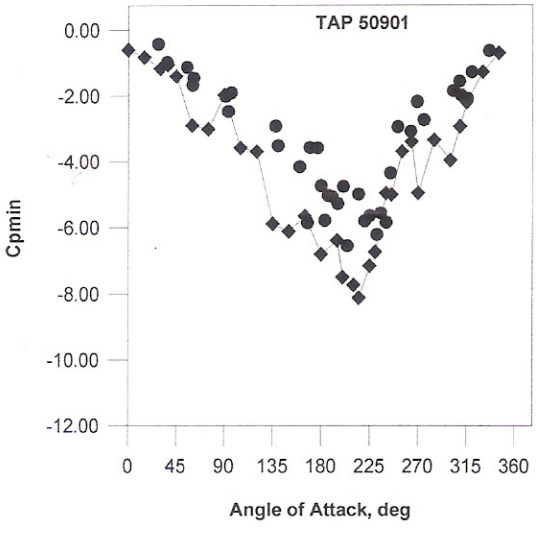

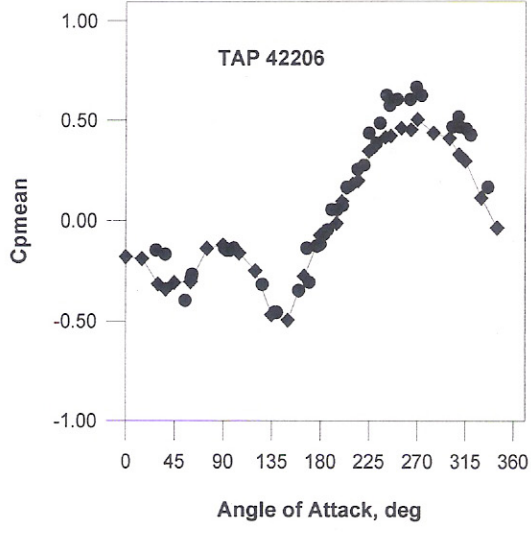

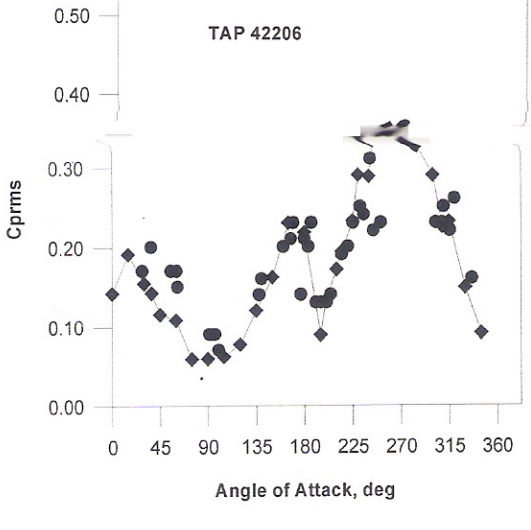

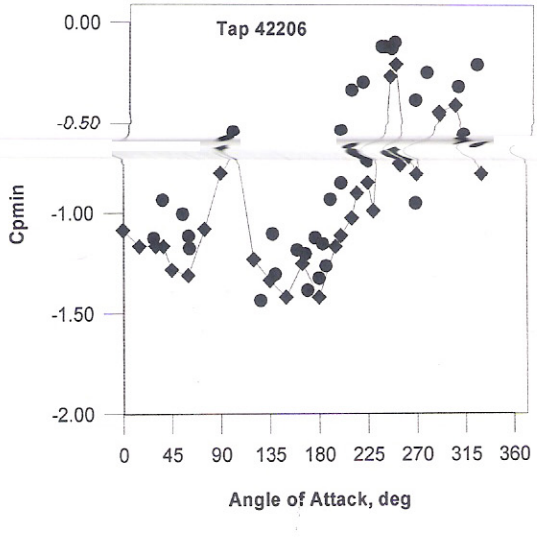

Fig 6 (d) TTU Building Cpmean, Cprms and Cpmin for Roof taps

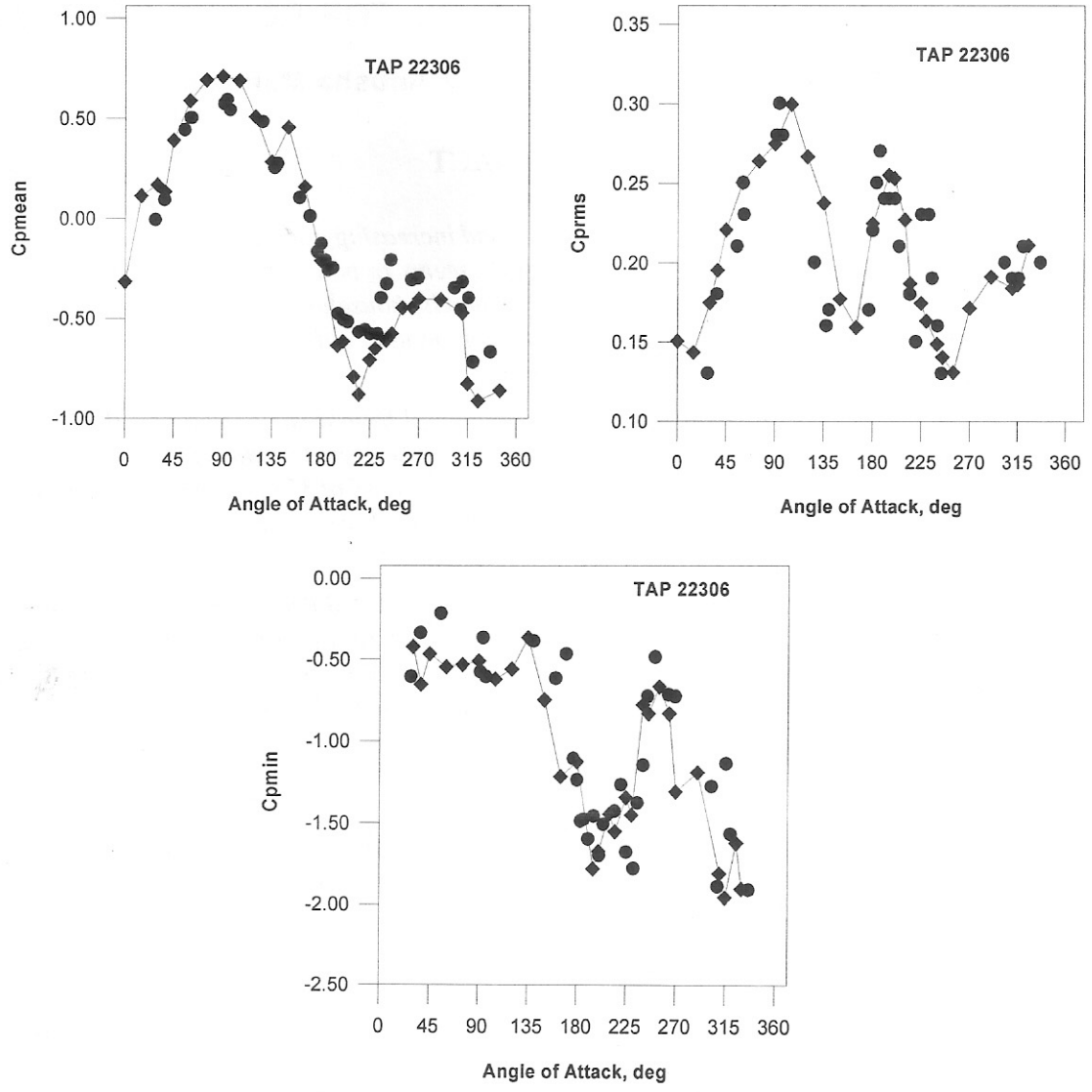

Fig 6 (e) TTU Building Cpmean, Cprms and Cpmin for Roof taps

Effect of Turbulence on the Pressure Coefficients

The full-scale data for Mode M04 showed considerable variation in the longitudinal turbulence levels, even for similar directions. Note the range from 15% to 25% and peak around 180° to 250°. Jamieson et al (1993) assessed the effect of this variation and showed that the reduction of velocity turbulence reduces the peak pressure coefficients significantly. This may be the main reason for the variation between the full-scale and wind tunnel pressure measurements for some wind directions for which the full-scale velocity turbulence is lower. Bienkiewicz and Ham (2003) also carried out tests for the effect of turbulence on the 1:50 scale TTU building model. The test results show significant increase in the pressure peaks and standard deviation with an increase in the flow turbulence.

CONCLUSION

On the basis of the work reviewed it has been established that for the wind tunnel studies on low-rise buildings, the atmospheric surface layer (ASL) should be modelled. Proper simulation of turbulence

intensities and small-scale turbulence content in the incident flow are required. Furthermore, exact scaling of the turbulence integral length scale does not seem essential for the prediction of the wind pressures on low-rise buildings. The study reconfirms some of the findings from previous studies.

ACKNOWLEDGEMENT

The work presented in this paper is part of the Ph. D. Thesis of the first author awarded in the Department of Civil Engineering I. I. T. Roorkee, Roorkee, India.

REFERENCES

1. Bienkiewicz, B., and Ham, H.J. (2003), "Wind tunnel modeling of roof pressure and turbulence effects on the TTU test building", *Journal of Wind and Structures, Vol. 6, No. 2, pp 91-106.*
2. Cheung, J.C.K., Holmes, J.D., Melbourne, W.H., Lakshmanan, N. and Bowditch, P. (1997), "Pressures on a 1/10 scale model of the Texas Tech Building", *Journal of Wind Engineering and Industrial Aerodynamics, Vol. 69-71, pp 529-538.*
3. Cook, N.J. (1978), "Determination of the model scale factor in wind-tunnel simulations of the adia batic atmospheric boundary layer", *Journal of Wind Engineering and Industrial Aerodynamics, Vol. 2, pp 311-321.*
4. Gupta, A. (1996), "Wind tunnel studies on aerodynamic interference in tall rectangular buildings", *Ph.D. Thesis, University of Roorkee, Roorkee, India.*
5. Jamieson, N.J., Carpenter, P., (1993), "Wind tunnel pressure measurements on the Texas Tech building at a scale of 1/25 and comparison with full scale", *7th U.S. National Conf. on Wind Engineering, Los Angeles, CA, Vol. I, pp 303-312.*
6. Mehta, K.C., Levitan, M.L., Iverson, R.E. and McDonald, J.R. (1992), "Roof corner pressure measured in the field on a low building", *Journal of Wind Engineering and Industrial Aerodynamics, Vol. 41-44, pp 181-192.*
7. Scruton, C. (1981), An Introduction to Wind Effects on Structures - Engineering Design Guides, *B.S.I. Oxford University Press.*
8. Simiu, E., and Scanlan, R.H., (1978), "Wind Effects on Structures", *John Wiley and Sons, New York*
9. Tieleman, H.W., Hajj, M.R., and Reinhold, T.A. (1998), "Wind tunnel simulation requirements to assess wind loads on low-rise buildings", *Journal of Wind Engineering and Industrial Aerodynamics, Vol. 74-76, pp 675-685.*
10. Tieleman, H.W., Reinhold, T.A. and Marshall, R.D. (1978), "On the wind-tunnel simulation of the atmospheric surface layer for the study of wind loads on low-rise buildings", *Journal of Wind Engineering and Industrial Aerodynamics, Vol. 3 pp 21-38.*
11. Tieleman, H.W., Reinhold, T.A., and Hajj, M.R. (1997), "Importance of turbulence for the prediction of surface pressures on low-rise structures", *Journal of Wind Engineering and Industrial Aerodynamics, Vol. 69-71, pp 519-528.*
12. Tieleman, H.W., Surry, D. and Mehta, K.C. (1996), "Full/model scale comparison of surface pressures on the Texas Tech experimental building", *Journal of Wind Engineering and Industrial Aerodynamics, Vol. 61, pp 1-23.*
13. Tieleman, HW., Hajj, M.R. and Reinhold, T.A. (1999), "Pressure characteristics for separated flows", *Wind Engineering into the 21st Century, Larsen, Larose & Livesey (Eds.), Balkema, Rotterdam, pp 1731-1738.*

Journal of Wind and Engineering, Vol. 8, No. 1, January 2011, PP. 23-42

WIND LOADS ON ROOFTOP EQUIPMENT MOUNTED ON A FLAT ROOF

James W. Erwin[1], Arindam Gan Chowdhury[2], Girma Bitsuamlak[3]

1 Research Scientist, CEE and IHRC, FIU, 11200 SW 8th Street, Miami, FL 33199, USA, jamerwin@fiu.edu
2 *Corresponding Author.* Assistant Professor, CEE, Director, Lab. for Wind Engineering Research, IHRC, FIU, 10555 W. Flagler Street, Miami, FL 33174, USA, chowdhur@fiu.edu
3 Assistant Professor, CEE and IHRC, FIU, 10555 W. Flagler Street, Miami, FL 33174, USA, bitsuamg@fiu.edu

ABSTRACT

Measurements of wind-induced loads on rooftop air conditioning (a/c) units were carried out at a full-scale testing facility. The a/c units were installed on the roof of a test building and instrumented with force and pressure transducers to capture the aerodynamic loading effects. The load coefficients were compared to those specified in the American Society of Civil Engineers (ASCE) Standard *Minimum Design Loads for Buildings and Other Structures*. The use of screens as a technique with the potential for mitigating wind loading on rooftop equipment was also investigated. Placing a porous metal screen around the rooftop equipment was found to reduce wind loading effects on the equipment by 33-70%, depending upon the porosity of the screen.

Key words : Wind load, rooftop equipment, mitigation, full-scale, gust factor

INTRODUCTION

Damage reconnaissance studies performed during the 2004 and 2005 Atlantic hurricane seasons identified rooftop equipment failures as one of the primary sources for millions of dollars worth of building damage, water infiltration, wind-borne debris, and delays in post-storm recovery due to the disruption of operations at critical recovery facilities (FEMA 488, 2005; FEMA 490, 2005). Of the four 2004 Florida hurricanes that caused the observed rooftop equipment-related damage, only Hurricane Charley produced wind speeds at or above design levels specified in the most recent editions of the Florida Building Code (FBC) and the International Building Code (IBC) (FEMA 490, 2005).

Following Hurricane Katrina in 2005, similar results were observed in Louisiana, Mississippi, and Alabama. The Katrina Mitigation Assessment Team (MAT) identified wind impacts to rooftop equipment as one area requiring further attention from designers, architects, and contractors (FEMA 549, 2006). This MAT also observed that rooftop equipment located on essential facilities, such as hospitals, police stations, and emergency operations centers, was generally not anchored any more securely than rooftop equipment found on common commercial structures. Similarly, damage assessments performed by the National Institute for Standards and Technology (NIST) in 2005 documented the impact of rooftop equipment failures, and the ensuing damages caused by wind-borne debris stemming from detached rooftop equipment (NIST Technical Note 1476, 2006).

These observations indicate that current rooftop equipment design criteria and anchorage methods may be inadequate to withstand severe winds. Primarily, this may be attributed to a lack of information on rooftop equipment design wind loadings. The objective of this study was twofold: to obtain realistic wind loading data for rooftop equipment by conducting full-scale experiments on typical roof-mounted air conditioning (a/c) units under simulated hurricane-force winds, and to develop and evaluate a mitigation technique that may alleviate the wind loading on existing rooftop equipment panels to improve their performance under extreme wind loads.

As a result of the extensive rooftop equipment failures observed in 2004 and 2005, Reinhold (2006) documented the procedures for calculating wind loading on rooftop equipment presented in American Society of Civil Engineers (ASCE) Standard *Minimum Design Loads for Buildings and Other Structures* (ASCE 7-02, 2003, ASCE 7-05, 2006), and offered designers provisional recommendations for the estimation of rooftop equipment wind loads until more research could be performed. Unlike earlier editions of the ASCE 7 Standard, ASCE 7-02 and ASCE 7-05 addressed rooftop equipment wind loads (section 6.5.13 in ASCE 7-02, and section 6.5.15 in ASCE 7-05), but only considered lateral forces. The ASCE 7-05 Commentary notes the existence of lift forces, but no formal procedure was given for their calculation, nor was there sufficient data on the possibility of increased loading caused by the equipment's position near higher uplift pressure zones around building corners and edges. The latest edition of the Standard, ASCE 7-10 (2010), includes Section 29.5.1 to address rooftop equipment uplift loading, in addition to lateral loading.

As rooftop equipment wind loading developed in the ASCE 7 Standard, a significant change was made between the ASCE 7-02 and the ASCE 7-05 methodologies through the addition of section 6.5.15.1 in ASCE 7-05, which governed the design of rooftop equipment placed on low-rise structures, defined as buildings with height h≤18.3 m (60 ft). This section required the lateral force, calculated by ASCE 7-05 Eqn. 6-28 (identical to ASCE 7-02 Eqn. 6-25)

$$F = q_z G C_f A_f , \tag{1}$$

to be multiplied by an additional factor of 1.9, which reduces linearly to 1.0 as the projected area of the rooftop equipment increases from less than or equal to 10% of the windward area of the building (i.e., 0.1B*h*) to 100% of the windward area of the building (i.e., 0.1B*h*), respectively, whereB is the building's width. Reinhold (2006) pointed out that, in general, the windward area of most rooftop equipment is less than 10% of the windward building area and, as a result, the factor of 1.9 is applicable to most rooftop equipment. This implies that for a majority of cases the ASCE 7-05 methodology resulted in a rooftop equipment lateral design force nearly two times greater than that calculated under the requirements of ASCE 7-02. The same methodology for calculating the lateral loading as prescribed in ASCE 7-05 has been continued in Section 29.5.1 of ASCE 7-10. In addition, ASCE 7-10 prescribes both lateral and uplift load coefficients (GCf and GC_r, respectively) for rooftop equipment mounted on low rise buildings. The increased design loads on rooftop equipment can be addressed by adequately designing the roof members and connection systems to support the equipment in the case of new construction. However, for existing buildings, the roof members might need extensive retrofitting/strengthening to support new pieces of rooftop equipment in order to address the increased design loading as per the new standard.

The changes to rooftop equipment wind loading made between ASCE 7-02 and ASCE 7-05 were based on the results of a wind tunnel investigation conducted by Hosoya et al. (2001),which modeled a 1.22 m x 1.22 m x 1.22 m (4 ft x 4 ft x 4 ft) a/c unit placed at three different locations on the roof of Texas Tech University's (TTU) Wind Engineering Research Field Laboratory (WERFL), at a scale of 1:50. This study

found that the highest measured surface pressures existed when the rooftop equipment was located near the edge of the base building and that the pressures decreased as the equipment was moved toward the center of the roof. The code modification was based on the study's findings that for the rooftop equipment configuration tested in the wind tunnel the peak gust factor G was 1.63, rather than the ASCE 7 nominal value of 0.85. To maintain a consistent nominal gust factor of 0.85 throughout the standard, an additional factor of 1.9 (1.63/0.85 = 1.9) was added in ASCE 7-05 to account for high pressure correlation on typical rooftop equipment units.

Small-scale wind tunnel experiments have proven essential in wind engineering. However, they may have limitations when modeling smaller components around the building envelope, such as rooftop equipment. Scaling restrictions, especially in terms of Reynolds number dissimilarity between small-scale and full-scale flows, make it difficult to reproduce detailed flow phenomena around smaller building components. Also, it is difficult to put a sufficient number of pressure taps on small-scale models of rooftop equipment because of size constraints, which may lead to reductions in accuracy of area averaged forces calculated using the pressure integration technique.

Field measurements on rooftop equipment are difficult for many reasons. Instrumenting rooftop equipment on real buildings without disrupting building operation or developing nonintrusive methods for installing sensors is challenging. Also, the probability of instrumented rooftop equipment units on a limited number of buildings experiencing sufficiently strong wind events is low and could require several years of waiting time. Although destructive testing methods such as vacuum chambers, reaction frames, and compressed air cannons have been used to simulate extreme wind-induced pressures, forces, and flying debris on full-scale structural components (Leatherman et al., 2007), difficulties would arise in the use of these testing methods for rooftop equipment because the dynamic lateral and uplift forces exerted on rooftop equipment are dependent not only upon the aerodynamic features of the equipment system, but also on the mounting configuration and the location on the base building.

LARGE- AND FULL-SCALE TESTING TECHNIQUES

Baker (2007) has pointed out the continuing need for large- and full-scale experimentation to confirm data obtained in wind tunnels and by computational fluid dynamics techniques. Full-scale testing of rooftop equipment is advantageous for several reasons. Force coefficients based on aerodynamic loads can be obtained directly from reaction forces measured for full-sized a/c units mounted in a realistic manner. This technique avoids pressure integration, the accuracy of which is highly dependent upon the spatial resolution of pressure measurements. Complex flow characteristics through louvers and openings found on real a/c units can be accounted properly; and testing real a/c units and mounting systems makes it possible to examine the structural integrity of the equipment and connections under simulated hurricane-force winds. Full-scale testing is especially advantageous for the part of this study related to mitigation devices, which contain perforations of critical functionality that are too small in size to be reproduced in wind tunnel model scale tests but can be prototyped without any distortion in fullscale tests.

Recognizing the need for full-scale wind loading information, wind engineers have recently developed several large- and full-scale testing facilities. The Three Little Pigs project at the University of Western Ontario uses actuators to create pressure distributions around full-scale building models based on pressure time histories measured in the wind tunnel (Kopp et al., 2006). The mobile wind simulator built by the University of Florida is a 2x4 fan array that has been used to evaluate the performance of low-rise building components and simulate winddriven rain based on data collected during land-falling tropical

cyclones (Lopez and Masters, 2010). The 6-fan Wall of Wind (WoW) large- and full-scale testing apparatus developed at Florida International University (FIU) has been successfully used to validate vortex suppression techniques to mitigate roof uplift pressures (Blessing et al., 2009). At the time of this study, at least two other full-scale testing facilities are in development: (1) the Institute for Business and Home Safety (IBHS) Research Center, expected to produce hurricane winds across a test section large enough to accommodate full-scale residential, commercial, and agricultural structures (Smith et al., 2010), and (2) the WindEEE dome at the University of Western Ontario, designed to simulate straight, shear, and swirl winds at large scales (http://www.eng.uwo.ca/windeee/facilities.html).

METHODOLOGY

Wall of Wind Facility

For the research described in this paper, full-scale experimentation of rooftop equipment wind loading was performed using the 6-fan WoW apparatus, located on the College of Engineering and Computing campus at FIU. Developed by the International Hurricane Research Center (IHRC), the 6-fan WoW is a 2x3 array of internal combustion engines and counterrotating transmissions that spin airboat propellers up to 2250 revolutions per minute (rpm). Prior to this study, the 6-fan WoW underwent modifications to the original configuration with the intent of improving critical flow parameters. Turbulence parameters of several real tropical cyclones were used as target parameters to simulate WoW flow characteristics as reported by Yu (2007), Yu et al. (2008) and Yu and Gan Chowdhury (2009). A combination of passive flow management devices and an active control system were implemented, making the 6-fan WoW capable of generating mean wind speed and turbulence characteristics similar to those of real tropical cyclones. The modified WoW apparatus is shown in Fig. 1. The 6-fan WoW testing apparatus is 4.9 m (16 ft) tall by 7.3 m (24 ft) wide and each test model is placed at a distance of 3 m (10 ft) from the WoW during testing.

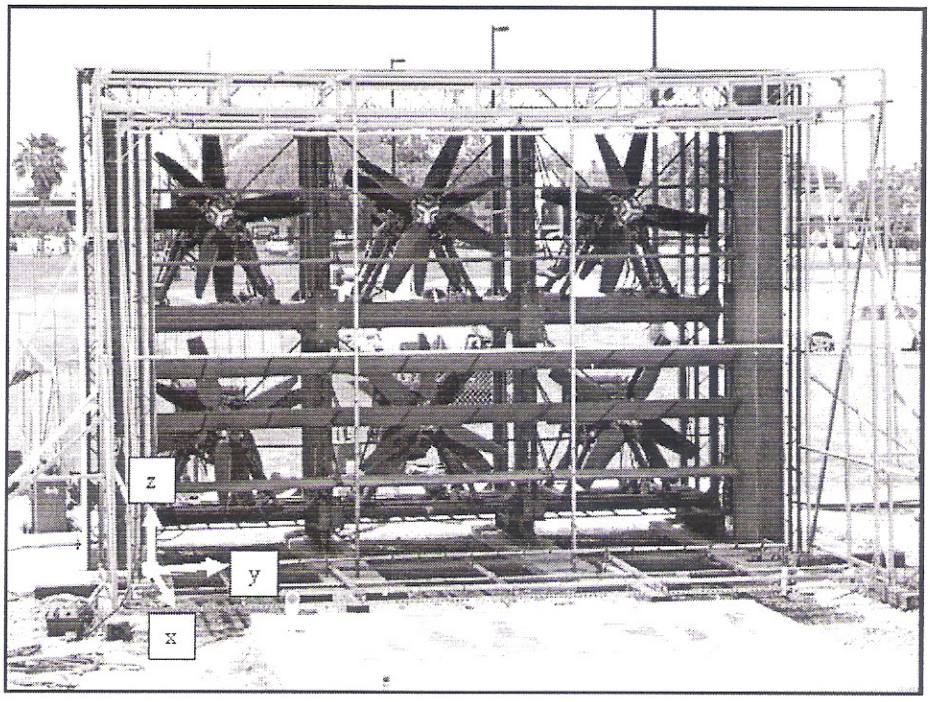

Fig. 1. Downwind view of the modified WoW apparatus.

The flow management devices allowed the modified 6-fan WoW to generate a suburban terrain mean wind profile (power law coefficient value α = 1/4.0) with 3-s gust wind speed of about 38 m/s at typical low-rise model roof eave height. The longitudinal and vertical turbulence intensities measured at the roof eave height were 24% and 7%, respectively. The integral length scale (L_u^x) at roof eave height was 90 m. For more detailed information on the modified 6-fan WoW configuration, its flow characteristics (including the wind turbulence spectra), and comparisons with tropical cyclone flow characteristics, see Huang, et al. (2009). For details on testing capabilities of the 6-fan WoW, see Blessing et al. (2009), Gan Chowdhury et al. (2009), Gan Chowdhury et al. (2009α), and Bitsuamlak et al. (2009).

It is to be noted that the "Wall of Wind" is a developing technology. Researchers at FIU are working in stages on the validation of the pressure fields generated on low-rise structures using the WoW open jet simulation. Blockage effects related to such open jet facilities have been studied by Dagnew et al. (2010). Currently, the researchers are working on measuring atmospheric boundary layer wind generated pressures on various configurations of low rise buildings (with monoslope, gable, and hip roofs) in a reputable boundary layer wind tunnel. The same models are being tested using 1:8 and 1:15 scale models of the WoW apparatus to facilitate comparison of pressures with those obtained from the wind tunnel. Open terrain wind profile development and initial pressure comparison results using a Silsoe cube model have been reported in Gan Chowdhury et al. (2010) and Aly et al. (2011). For the current research, the 6-fan WoW apparatus was used. However, the current test results are considered as preliminary findings. Future research will be performed at the WoW facility to compare the drag coefficients obtained on cubical structures (similar to rooftop a/c equipment) in the absence of the building underneath to facilitate comparisons with well-established drag coefficients in a free stream in the literature. In addition, 'quasi-periodic' waveforms for generating turbulence will be further improved in the future to better simulate atmospheric turbulence parameters, which would improve measured load time histories.

Full-Scale Measurement of Rooftop Equipment Wind Loads

For this research, a representative a/c condenser (Rheem model RAND-024JAZ) rooftop equipment was used. The components and materials used were consistent with current design schedules approved by the Florida Building Code (FBC) and the Miami-Dade County Building Code Compliance Office (BCCO) at the time of the study. Three a/c condenser units, each having dimensions of 0.9 m x 0.7 m x 0.5 m (3.25 ft x 2.30 ft x 1.58 ft), were mounted on a 2.7 m x 0.69 m x 0.61 m (9 ft x 2.25 ft x 2 ft) aluminum a/c stand with six legs (Fig. 2). Placing multiple a/c units on a single frame is a typical configuration found on many

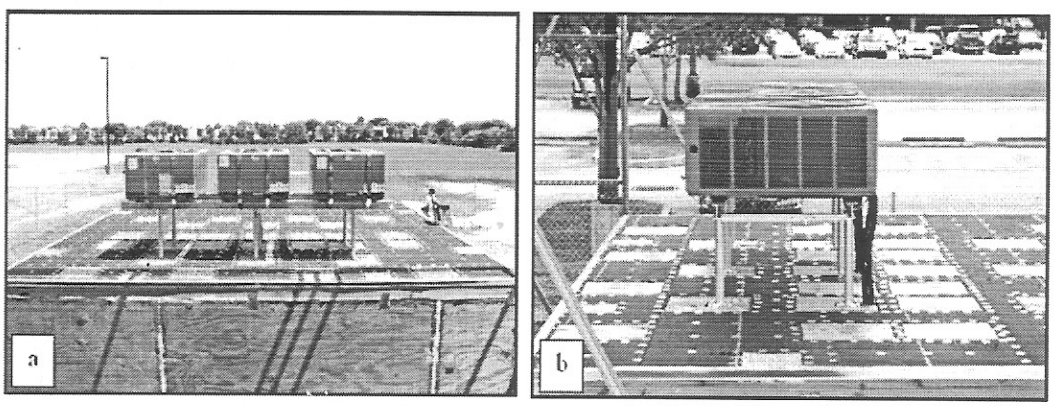

Fig. 2. Rooftop equipment used in this study: three a/c condenser units mounted on an aluminum a/c stand; (a) upwind view, (b) side view.

low-rise buildings in South Florida. Four rubber vibration isolators were placed between each a/c unit and the aluminum stand. The a/c units were secured to the stand with continuous pieces of 25.4 mm (1 in) wide galvanized steel strap wrapped around the a/c units and mechanically attached to the aluminum stand with appropriately sized sheet metal screws. The base building dimensions were chosen to ensure that the rooftop equipment's windward projected area (A_f) and the projected area of the top surface (A_r) would be less than 10% of the building's windward wall area and roof area, respectively. Based on these criteria, a flat-roofed wooden base building was constructed measuring 2.4 m (8 ft) tall and 4.9 m (16 ft) wide in both horizontal dimensions. Ratios of $A_{f,equip}/A_{f,bldg}$ = 8.5% and $A_{r,equip}/A_{r,bldg}$ = 8.8% were achieved with this setup.

The rooftop equipment was tested at two different locations on the base building: near the roof edge (Fig. 3a) and at the middle of the roof (Fig. 3b). The full-scale testing was performed with wind applied at a 0^0 angle of attack (perpendicular to the roof edge), based on the results of Hosoya et al. (2001), which demonstrated that the largest lateral force coefficients occurred when the wind was acting approximately normal to the rooftop equipment model. Although Hosoya et al. (2001) found the highest uplift force coefficient occurred under diagonally approaching winds, oblique wind directions were not considered for the current study and testing under different wind angles of attack will be performed in the future.

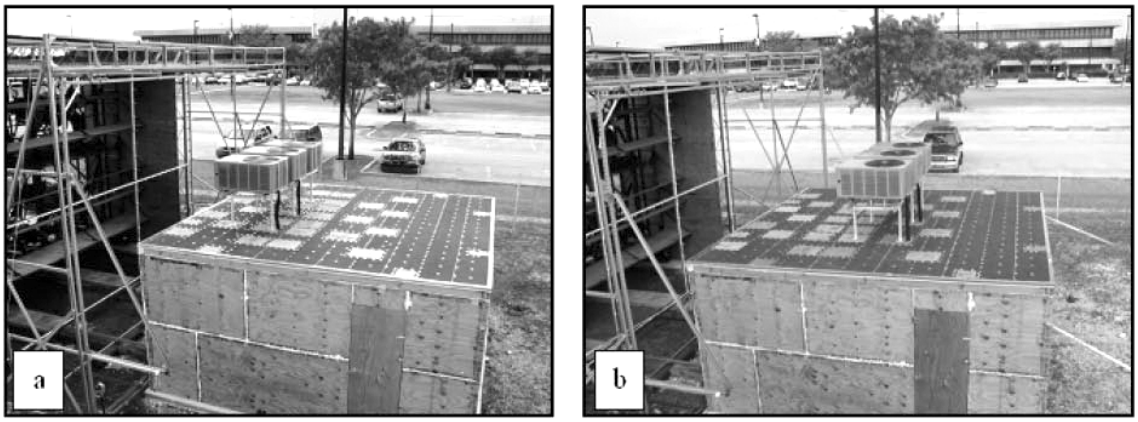

Fig. 3. Rooftop equipment testing locations on the base building: (a) roof edge, and (b) middle of the roof.

Rectangular bays measuring 0.4 m (16 in) long x 0.3 m (12 in) wide were built beneath the roof surface of the base building (Fig 4), providing a place to conceal the load cells so they would not affect the flow across the roof, or raise the height of the rooftop equipment above the roof. The bays were located on the roof at the corresponding attachment points for the a/c stand base plates. During the experiments, plywood panels were installed above the instrumentation bays, flush with the roof surface, to protect the load cells from wind and to simulate a flat roof surface. Custom mounting devices were designed and fabricated to measure the lateral and vertical forces beneath each base plate. Each mount was built on a linear motion system consisting of a THK model HSR35B guide block and a 280 mm (11 in) rail. The linear motion system was chosen because it provided bending moment-resistance, and ensured that lateral forces would be transferred to the load cells with minimal friction losses. An Omega LC402-2k pancake-type load cell measured the vertical force beneath each leg of the a/c stand, and an Omega LC101-2k S-type load cell measured the lateral force. A 25.4 mm (1 in) thick aluminum adapter plate joined both load cells to the guide block by bolts. A 127 mm x 127 mm x 19 mm (5 in x 5 in x ¾ in) aluminum plate was bolted to the top of the LC-402 load cell to create a method for attaching the a/c stand to the instrumented mounting device using the standard mounting holes in the base plate. In addition to the force sensors, a total of 32 pressure taps were

placed on two of the a/c units (the middle unit and one side unit) to measure the external surface pressures during the experiments. Setra 265 differential pressure transducers measured the time-varying pressure for each tap.

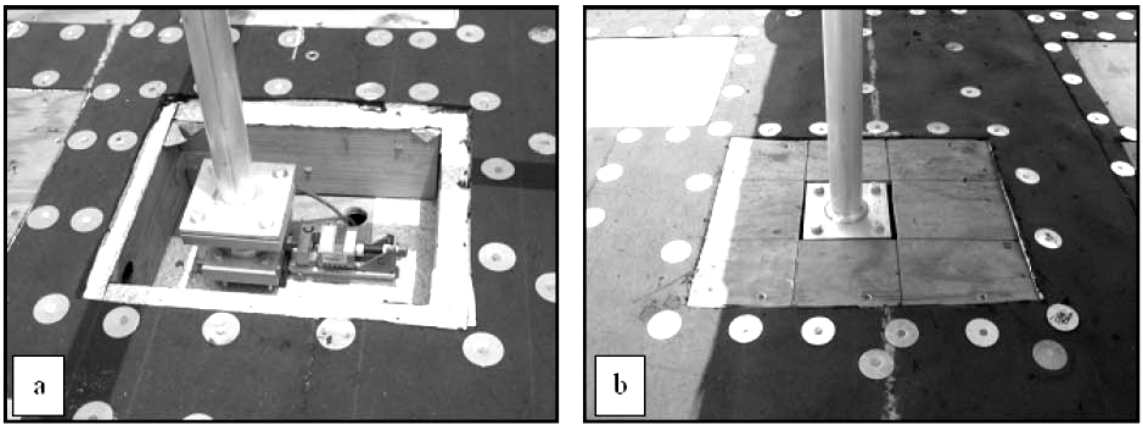

Fig. 4. Instrumentation mounting details on the base building roof: (a) view with plywood panel removed, providing access to the force transducers, and (b) view of the final setup during the experiments.

Mitigation Approach: Porous Screens

For the rooftop equipment configuration chosen for this study at least three possible failure modes exist: (1) the panels on the a/c units may detach, (2) the a/c units may detach from the aluminum stand, and (3) the a/c stand may detach from the roof of the base building. It is challenging to develop a single mitigation technique that would alleviate all of these potential failure modes. For example, connection details can be modified to improve safety with respect to the a/c stand detachment from the roof of the base building. However, this will not alleviate aerodynamic loading on the a/c unit panels and therefore not prevent panel failure under high winds.

For this study a mitigation technique using porous screens was tested. Many studies have reported the sheltering effect and feasibility of using porous screens (also called "fences" or "windbreaks") to mitigate unfavorable wind effects in various applications (e.g.: Fang and Wang, 1997; Yaragal et al, 1997; Lee and Park, 1998; Lee and Kim, 1999; Dong et al., 2007; Kang et al., 2007; Loredo-Souza et al., 2007; and Santiago et al., 2007). Based on these findings it was determined that a porous screen mitigation device may be developed to shelter rooftop equipment during extreme winds, thereby reducing the aerodynamic loads exerted on the rooftop equipment panels, and effectively reducing the likelihood of panel failures. The reduced aerodynamic loading will also help in alleviating the other identified modes of failure.

A steel frame was constructed to support porous metal screens around the rooftop equipment. The frame measured 3.4 m (11 ft) wide by 1.7 m (5.5 ft) deep, providing at least 0.3 m (1 ft) of clearance between the wind screens and the a/c units in both horizontal directions. The porous screens were 0.61 m (2 ft) high, and were raised above the roof surface by 0.58 m (1.92 ft). Four different types of metal screens were chosen for the study (Fig. 5), and porosities of approximately 35% and 63% were selected based on effective porosities found in wind tunnel studies (e.g. Kang et al., 2007; Loredo-Souza et al., 2007; Santiago et al., 2007). The details of each screen are:

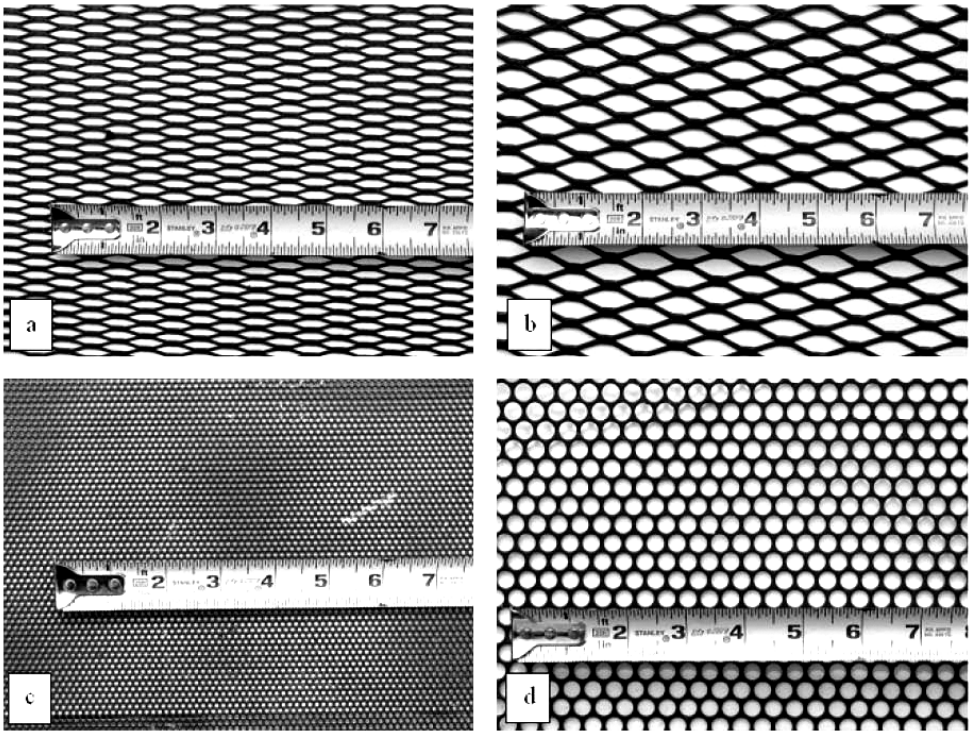

Fig. 5. Porous screens tested during the wind screen mitigation study: (a) screen 1, (b) screen 2, (c) screen 3, and (d) screen 4.

1. *Screen 1*: 0.9 mm (20 Ga) expanded metal, 6.4 mm (0.25 in) gap, flattened mesh, 35% porosity
2. *Screen 2*: 1.5 mm (16 Ga) expanded metal, 12.7 mm (0.5 in) gap, flattened mesh, 63% porosity
3. *Screen 3*: 1.5 mm (16 Ga) perforated metal, 2.0 mm (5/64 in) holes on 3.1 mm (1/8 in) centers, staggered pattern, 35% porosity
4. *Screen 4*: 1.5 mm (16 Ga) perforated metal, 7.9 mm (5/16 in) holes on 9.5 mm (3/8 in) centers, staggered pattern, 63% porosity

The porous screens were secured to the steel frame with bolts, making them easy to interchange. Fig. 6 shows the wind screen installed around the rooftop equipment at the roof edge and at the middle of the roof.

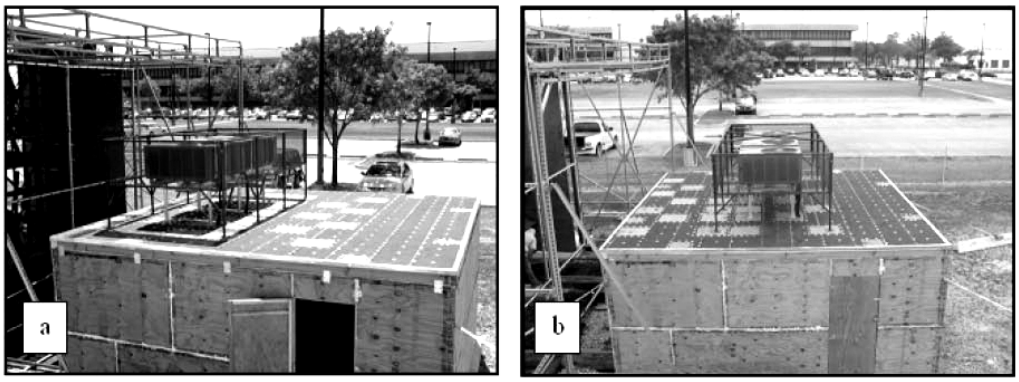

Fig. 6. Wind screen mitigation installed around the rooftop equipment: (a) roof edge, and (b) middle of the roof.

Experimental Procedures

WoW experiments were performed using quasiperiodic waveform signals controlling fan speed, developed by Huang et al. (2009) to generate wind turbulence characteristics. The largest lateral loads measured in the wind tunnel occurred when the rooftop equipment was nearly normal to the oncoming flow (Hosoya et al., 2001). Therefore, in the WoW experiments the wind direction was normal to the rooftop equipment and the base building. During each experiment, force and pressure data were sampled for 3-min at a rate of 100 Hz. Prior to running the WoW apparatus, baseline measurements were recorded to consider initial loading conditions on the sensors so the wind-induced forces and pressures could be determined by data postprocessing.

For testing at both locations atop the base building, a control test was performed first, in which the aerodynamic loads on the rooftop equipment setup were measured. Following the control test, the porous screen mitigation device was installed around the rooftop equipment setup, with screen 1 attached. The wind-induced loads on the rooftop equipment setup were then measured with the mitigation device in place. This process was repeated for the three remaining screens.

Data Analysis Procedures

A simplified, 2-dimensional free body diagram illustrating the external forces acting on the rooftop equipment setup is shown in Fig. 7. The terms F_x, F_z, and M_y represent the aerodynamic shear, uplift, and overturning moment exerted on the rooftop equipment, respectively. Reactions S_1, V_1, and M_1 indicate the respective total shear force, vertical force, and overturning moment on the leeward portion of the a/c stand. Likewise, reactions S_2, V_2, and M_2 denote the respective total shear force, vertical force, and overturning moment on the windward portion of the a/c stand. The term W represents the gross weight of the rooftop equipment, which was assumed to act at the geometric center of the a/c units, distance d denotes the center-to center width between the legs on the a/c stand, and distance H denotes the height of the a/c stand above the roof surface. Distances h and c represent the lever arms for F_x and F_z, respectively, which are time-varying quantities dependent upon the instantaneous velocity of the oncoming wind.

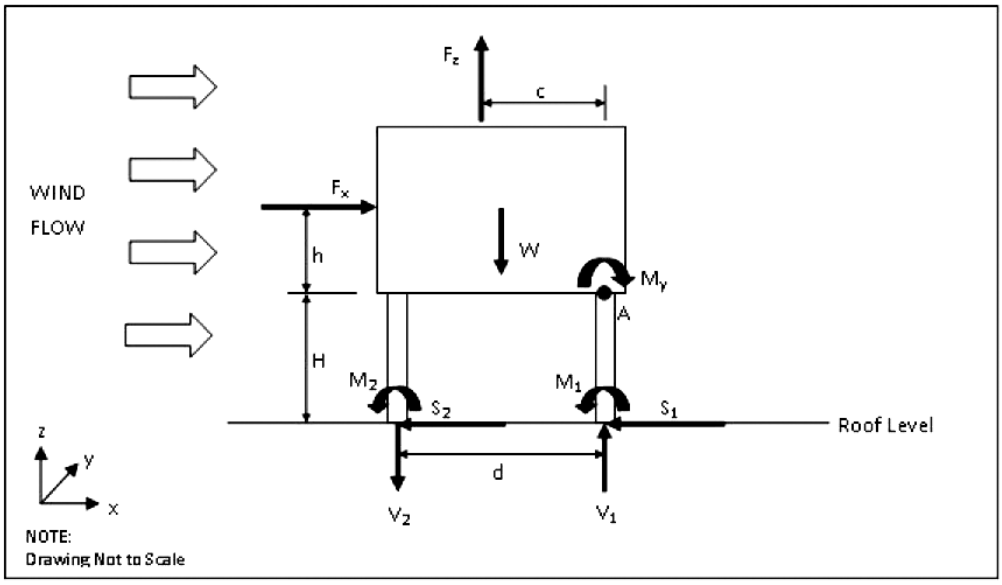

Fig. 7. Two-dimensional free body diagram of the rooftop equipment.

The aerodynamic forces acting on the rooftop equipment at any instant, F_x and F_z, may be determined by summation of the instantaneous lateral and vertical forces measured under each base plate on the a/c stand, according to the following equations:

$$F_x = \sum_{i=1}^{6} s_i \tag{2}$$

$$F_z = \sum_{i=1}^{6} v_i - W \tag{3}$$

Since the load cells used in this study were unable to measure the individual moment reactions beneath each base plate, the overturning moment exerted on the rooftop equipment system, *My*, was determined mathematically by summing moments about point *A*:

$$F_z \cdot c + F_x \cdot h - W \cdot \frac{d}{2} + (S_1 + S_2) \cdot H - V_2 \cdot d - M_1 - M_2 = 0 \tag{4}$$

From Hosoya et al. (2001), the aerodynamic moment, M_y, may be expressed in terms of the aerodynamic lateral and uplift forces according to the following expression:

$$M_y = F_x.h + F_z.c \tag{5}$$

Substituting Eqn. 5 into Eqn. 4 yields:

$$M_y = W \cdot \frac{d}{2} - (S_1 + S_2) \cdot H + V_2 \cdot d + M_1 + M_2 \tag{6}$$

The reaction moments M_1 and M_2 may be derived from a static analysis of the 2-dimensional free body diagram. Assuming the a/c units were attached rigidly to the aluminum stand and the bases of the a/c stand were fixed to the roof members, the following expression may be written:

$$M_1 = M_2 = \frac{F_x H}{2} \tag{7}$$

Substituting Eqn. 7 into Eqn. 6 gives an expression for M_y independent of the unknown distances *c* and *h*:

$$M_y = W \cdot \frac{d}{2} - (S_1 + S_2) \cdot H + V_2 \cdot d + (\frac{F_x}{2} + \frac{F_x}{2}) \cdot H \tag{8}$$

By noting that $F_x = S_1 + S_2$, Eqn. 8 may be further simplified to:

$$M_y = W \cdot \frac{d}{2} + V_2 \cdot d \tag{9}$$

RESULTS AND DISCUSSION

Aerodynamic Loading Effects

Figure 8 shows the 3-min time histories for F_x, F_z, and M_y when the equipment was placed near the roof edge. These time histories contain peak values that are random in nature and are therefore characterized by probability distributions. Peaks were estimated for a 1-hr storm duration using the method developed by Sadek and Simiu (2002). A 95% confidence level was chosen for the sake of conservatism. Summaries of the observed mean, root mean squares (RMS), peak, and the estimated 1-hr peak values for F_x, F_z, and M_y are given in Tables 1-3. Results indicate that the largest measured and estimated wind loads occurred when the rooftop equipment was placed near the roof edge, consistent with the wind tunnel findings in Hosoya et al. (2001), and the assertion by Reinhold (2006) that increased loading on rooftop

equipment is expected when the equipment is placed in a region of flow separation. It is to be noted that the values given in Tables 1-3 for F_x, F_z, and M_y are obtained for the entire set-up of the three a/c units. Such an approach was considered based on the assumption of more or less uniform distribution in loading across the width of the entire setup due to symmetry. However, in the future, a statistical analysis will be performed for loading transferred to individual legs to validate this assumption.

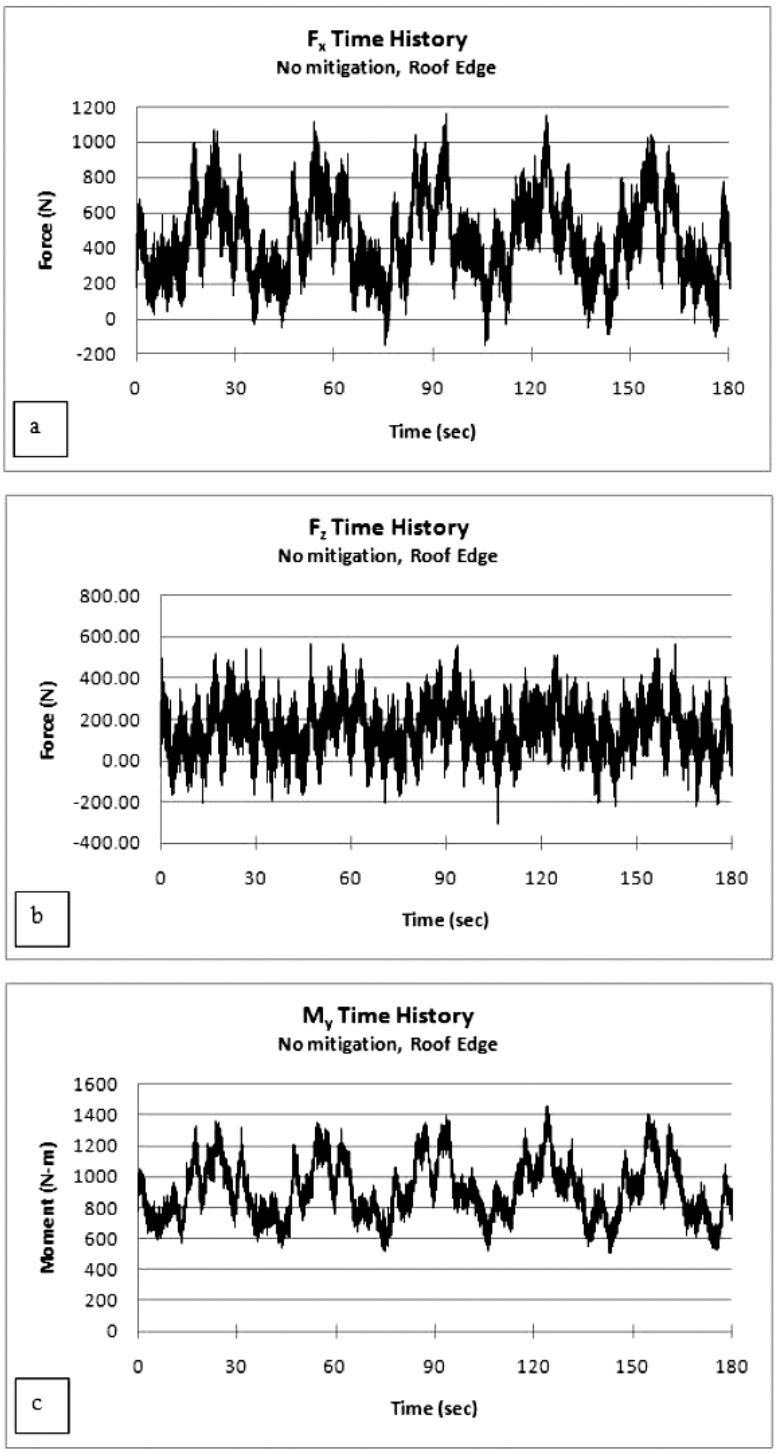

Fig. 8. Time histories of the aerodynamic rooftop equipment loads measured at the roof edge: (a) *Fx*, (b) *Fz*, (c) *My*.

Table 1. Observed 3-min and estimated 1-hr rooftop equipment lateral load, *Fx*

Rooftop equipment location	No mitigation							
	Observed (3 min)						Estimated $F_{x,max}$ (1 hr)	
	$F_{x,mean}$ N [lbs]		$F_{x,RMS}$ N [lbs]		$F_{x,max}$ N [lbs]		P = 0.95 N [lbs]	
Edge of Roof	447.9	[100.7]	222.4	[50.0]	1160.5	[260.9]	1897.8	[426.6]
Middle of Roof	413.7	[93.0]	193.8	[43.6]	1029.5	[231.4]	1728.2	[388.5]

Table 2. Observed 3-min and estimated 1-hr rooftop equipment uplift load, *Fz*

Rooftop equipment location	No mitigation							
	Observed (3 min)						Estimated $F_{z,max}$ (1 hr)	
	$F_{z,mean}$ N [lbs]		$F_{z,RMS}$ N [lbs]		$F_{z,max}$ N [lbs]		P = 0.95 N [lbs]	
Edge of Roof	147.2	[33.1]	114.6	[25.8]	569.4	[128.0]	962.4	[216.3]
Middle of Roof	90.7	[20.4]	95.1	[21.4]	469.8	[105.6]	907.8	[204.1]

Table 3. Observed 3-min and estimated 1-hr rooftop equipment overturning moment, *My*

Rooftop equipment location	No mitigation							
	Observed (3 min)						Estimated $M_{y,max}$ (1 hr)	
	$M_{y,mean}$ N-m [lb-ft]		$M_{y,RMS}$ N-m [lb-ft]		$M_{y,max}$ N-m [lb-ft]		P = 0.95 N-m [lb-ft]	
Edge of Roof	909.3	[670.7]	182.8	[134.8]	1457.5	[1075.0]	2112.6	[1558.2]
Middle of Roof	850.1	[627.0]	165.8	[122.3]	1376.3	[1015.1]	1978.0	[1458.9]

WoW results were compared to the ASCE 7-05 design wind loading by solving for the term GC_f in Eqn. 1, considering the WoW estimated 1-hr peak forces as the design wind load. To be consistent with the standard, the mean dynamic pressure (q) was calculated at the height corresponding to the centroid of the windward area of the a/c units tested in this study, approximately 3.35 m (11 ft) above ground level. At this height, a free-stream 3-min mean wind speed of 22.6 m/s (~50 mph) was measured across the hori zontal span of the rooftop equipment using the WoW quasiperiodic waveform developed by Huang et al. (2009). It is noted that this calculation differs slightly from the wind tunnel study of Hosoya et al. (2001), which considered the mean dynamic pressure measured at the roof eave height of the base building. Because ASCE 7-05 defines the 3-sec gust as the reference design wind speed, the observed WoW 3-min mean wind speed must be converted to a 3-sec gust wind speed. The Durst curve is commonly used to convert wind speed averaging times in atmospheric flows, but specifically corresponds to wind flowing over open terrain at elevation z = 10 m (32.8 ft). Consequently, the Durst curve is not applicable to WoW-generated flows. Instead, the gust factor curve reported in Huang et al. (2009, Fig. 13) was used to obtain the following

conversion factors for time-averaging WoW flows: $U_{3s} / U_{180s} = 1.43$ and $U_{180s} / U_{360s} = 1.04$. Combining these terms, a relationship between the 3-min wind speed and the 3-sec gust is found:

$$\frac{U_{3s\,WoW}}{U_{180s\,WoW}} = 1.38 \tag{10}$$

Thus, the 3-s gust wind speed is found to be 31.2 m/s (~70 mph) for this study.

Using a 3-s gust reference basis, the peak 1-hr lateral and uplift force coefficients arefound from Eqn. 1 to be $GC_f = 3.1$ and $GC_r = 0.75$, respectively. For lateral loading, this study shows that the peak is significantly higher than GC_f value of 2.1 as determined by Hosoya et al. (2001), which is essentially the same value implied in ASCE 7-05 (2.1 is the product of the gust effect factor of 0.85, the baseline lateral force coefficient of 1.3 found in Fig 6-21 of the standard, and the additional factor of 1.9 for smaller-sized rooftop equipment). This result indicates that ASCE 7-05 may underestimate the lateral wind loading on rooftop equipment by as much as approximately 50%. It is anticipated that GC_f value would be reduced linearly from 3.1 to 1.1 as the value of A_f is increased from (*0.1Bh*) to (*Bh*); however, more research is needed to validate this through testing using various ratios between the rooftop equipment's windward projected area (A_f) and the building's windward wall area (*Bh*).

The uplift coefficient measured in this study was lower than the peak wind tunnel result of 1.6, and may be attributed to raising the a/c units above the roof surface, a more realistic configuration for smaller a/c units. Mounting the equipment in this manner causes counteracting suctions on the top and bottom surfaces of the equipment, lessening the net uplift pressure. Time histories of panel forces (follow ing the same sign conventions as shown in Fig. 7), calculated by pressure integration of taps located on the top and bottom surfaces of the middle a/c unit, provide evidence of this phenomenon (Fig 9) and produce an uplift coefficient approximately one-half of that measured in the wind tunnel study, which had the equipment mounted flush with the roof surface. Since rooftop equipment mounting requirements vary in terms of space between the equipment and the roof, the wind tunnel results appear to be conservative. However, it is recommended that the uplift design load coefficients[4] in ASCE 7-10, based on the wind tunnel results, be used until more extensive research is performed. Since this study only considered a specific gap between the equipment and the roof, further work is needed to investigate the effects of various gaps on the reduction in net uplift for various wind directions.

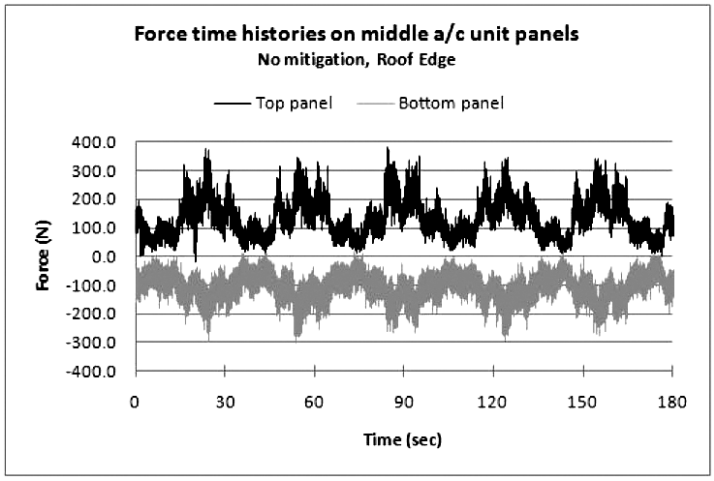

Fig. 9. Uplift time histories on the middle a/c unit showing opposing forces acting on the top panel and bottom panel.

[4] GC_r, ranging from 1.5 to 1.0 based on the ratio between the horizontal projected area of the equipment (A_r) versus the horizontal projected area of the roof

Based on the aerodynamic moment results listed in Table 3, it is likely that aerodynamic moments contribute significantly to rooftop equipment detachment, although the magnitude of the overturning moment is dependent on the mounting conditions and may vary considerably for different shapes, sizes, and configurations of rooftop equipment. Due to the mounting conditions used in this study, the aerodynamic moment cannot be simply calculated by using Eqn. 5 under the assumptions that the peak lateral force and uplift force occur simultaneously and act at the geometric centers of the rooftop equipment height and width, respectively. This is further indicated as the 1-hr peak aerodynamic overturning moment of 787.9 N-m calculated using Eqn. 5 is significantly less than its counterpart estimated using Eqn. 9 (shown as 2112.6 N-m in Table 3 for the roof edge), which is independent of the unknown distances *h* and *c*. This difference could be due to two possible reasons: Firstly, the peak lateral force could act at a point higher than the midpoint of the frontal face and the peak uplift force could act at a point closer to the windward edge; in which case the higher values of *h* and *c* would give higher aerodynamic overturning moment M_y using Eqn. 5 compared to the case where the peak lateral and uplift forces were assumed to act at the geometric centers of the rooftop equipment. Secondly, the reaction moments M_1 and M_2 were estimated in Eqn. 7 by assuming a full fixity condition; however, in general, full fixity is not achieved, in which case lower reaction moments and lower aerodynamic overturning moment M_y will be obtained using Eqns. 6 through 9. Due to the limited number of pressure taps used during the current testing, the aerodynamic overturning moment was not estimated from pressure time histories. Evaluation of high overturning moments in this study suggests that the development of overturning moment criteria might be necessary. However, further testing should be done to directly measure overturning moments on a variety of shapes, sizes, and mounting configurations before the need for such criteria is definitively established.

Wind Screen Mitigation Results

Tables 4-6 show the observed 3-min and estimated 1-hr aerodynamic reactions measured for the rooftop equipment while the wind screen mitigation device was installed. The measured reaction forces indicate that the wind screens significantly reduced the overall aerodynamic effects on the rooftop equipment. Screen 3 consistently demonstrated the greatest sheltering effect among the four screens tested, yielding the highest reductions in the peak 1-hr estimated values of F_x, F_z, and M_y ranging from 56-69% at both the roof edge and the middle of the roof. The remaining screens also performed well, showing aerodynamic load reductions ranging from approximately 30-60%. Following Screen 3, Screen 1 showed higher reductions than Screens 2 and 4, indicating that the screens with 35% porosity were more effective than the ones with 65% porosity. It may be noted that the geometry of the porous screen openings did not exhibit a significant impact on screen performance as the two screens with the same porosity but with different opening configuration produced similar results.

Table 4. Comparison of observed 3-min and estimated 1-hr peak lateral force *Fx* with wind screen mitigation

Rooftop equipment location	Test Case	Wind screen mitigation										% Reduction of 1 hr peak estimated load versus no mitigation
		Observed (3 min)						Estimated $F_{x,max}$ (1 hr)				
		$F_{x,max}$ N [lbs]		$F_{x,RMS}$ N [lbs]		$F_{x,max}$ N [lbs]		P = 0.95 N [lbs]				
Edge of Roof	Screen 1	210.4	[47.3]	131.1	[29.5]	755.9	[169.9]	1118.2	[251.4]			41%
	Screen 2	283.4	[63.7]	138.6	[31.2]	742.2	[166.9]	1209.9	[272.0]			36%
	Screen 3	118.8	[26.7]	93.3	[21.0]	530.9	[119.4]	826.3	[185.8]			56%
	Screen 4	258.0	[58.0]	144.3	[32.4]	797.3	[179.2]	1276.7	[287.0]			33%
Middle of Roof	Screen 1	171.7	[38.6]	94.0	[21.1]	541.9	[121.8]	818.5	[184.0]			53%
	Screen 2	258.4	[58.1]	114.2	[25.7]	732.6	[164.7]	1028.8	[231.3]			40%
	Screen 3	113.0	[25.4]	67.9	[15.3]	469.6	[105.6]	612.3	[137.7]			65%
	Screen 4	281.1	[63.2]	118.9	[26.7]	730.8	[164.3]	1057.4	[237.7]			39%

Table 5. Comparison of observed 3-min and estimated 1-hr peak uplift force *Fz* with wind screen mitigation

Rooftop equipment location	Test Case	Wind screen mitigation								% Reduction of 1 hr peak estimated load versus no mitigation
		Observed (3 min)						Estimated $F_{z,max}$ (1 hr)		
		$F_{z,mean}$ N [lbs]		$F_{z,RMS}$ N [lbs]		$F_{z,max}$ N [lbs]		P = 0.95 N [lbs]		
Edge of Roof	Screen 1	-82.7	[-18.6]	88.0	[19.8]	298.2	[67.0]	446.2	[100.3]	54%
	Screen 2	25.4	[5.7]	77.6	[17.5]	364.4	[81.9]	496.6	[111.6]	48%
	Screen 3	-40.5	[-9.1]	77.5	[17.4]	305.5	[68.7]	427.1	[96.0]	56%
	Screen 4	35.6	[8.0]	84.7	[19.0]	404.1	[90.8]	545.4	[122.6]	43%
Middle of Roof	Screen 1	28.9	[6.5]	57.9	[13.0]	349.5	[78.6]	384.8	[86.5]	58%
	Screen 2	3.6	[0.8]	61.5	[13.8]	274.9	[61.8]	380.5	[85.5]	58%
	Screen 3	-56.0	[-12.6]	54.7	[12.3]	253.8	[57.1]	280.8	[63.1]	69%
	Screen 4	11.6	[2.6]	63.8	[14.3]	313.1	[70.4]	401.7	[90.3]	56%

Table 6. Comparison of observed 3-min and estimated 1-hr peak uplift force *My* with wind screen mitigation

Rooftop equipment location	Test Case	Wind screen mitigation								% Reduction of 1 hr peak estimated load versus no mitigation
		Observed (3 min)						Estimated $M_{y,max}$ (1 hr)		
		$M_{y,mean}$ N [lb-ft]		$M_{y,RMS}$ N [lb-ft]		$M_{y,max}$ N [lb-ft]		P = 0.95 N [lb-ft]		
Edge of Roof	Screen 1	624.4	[460.5]	71.4	[52.7]	889.8	[656.3]	1108.3	[817.5]	48%
	Screen 2	712.6	[525.6]	91.9	[67.7]	1020.6	[752.8]	1335.7	[985.2]	37%
	Screen 3	552.9	[407.8]	39.4	[29.0]	777.4	[573.4]	824.9	[608.4]	61%
	Screen 4	725.2	[534.9]	95.0	[70.1]	1063.4	[784.3]	1399.7	[1032.4]	34%
Middle of Roof	Screen 1	664.1	[489.8]	58.5	[43.2]	914.3	[674.4]	1074.2	[792.3]	46%
	Screen 2	659.9	[486.7]	78.5	[57.9]	939.6	[693.0]	1178.3	[869.1]	40%
	Screen 3	545.2	[402.1]	27.1	[20.0]	722.5	[532.9]	771.5	[569.1]	61%
	Screen 4	685.9	[505.9]	83.0	[61.2]	1002.6	[739.5]	1274.1	[939.7]	36%

As stated earlier, although strengthening the connections between the a/c units, the aluminum frame, and the base building may be an alternative approach to increasing the performance of rooftop equipment in extreme winds, strengthening these connections will not address all of the potential failure modes and hazards associated with rooftop equipment losses, especially panel failures. The wind screen mitigation concept may be advantageous for various reasons: (1) The sheltering effect of the wind screen reduces the aerodynamic loading on the rooftop equipment, thereby reducing the likelihood of panels detaching from the equipment itself and becoming wind-borne debris. This reduction in panel forces, calculated using pressure integration, is clearly shown by comparing force time histories on each surface of the middle a/c unit, with and without the presence of a wind screen (Fig. 10, following the same load sign conventions as shown in Fig. 7); (2) If designed to sustain a reasonable impact, the wind screens may protect the rooftop equipment

from wind-borne debris impacts, reducing the risks of panel failure and complete detachment of the equipment; (3) The wind screen alternative would be most useful on existing buildings in which no other retrofitting alternative could be implemented. For example, if a new piece of rooftop equipment is designed for installation on a structure built according to design standards prior to ASCE 7-05, installation of the wind screen could prevent the need for special structural details to strengthen the members receiving the new rooftop equipment loads. However, further research is needed to evaluate the loading on various roof members with and without the mitigation device.

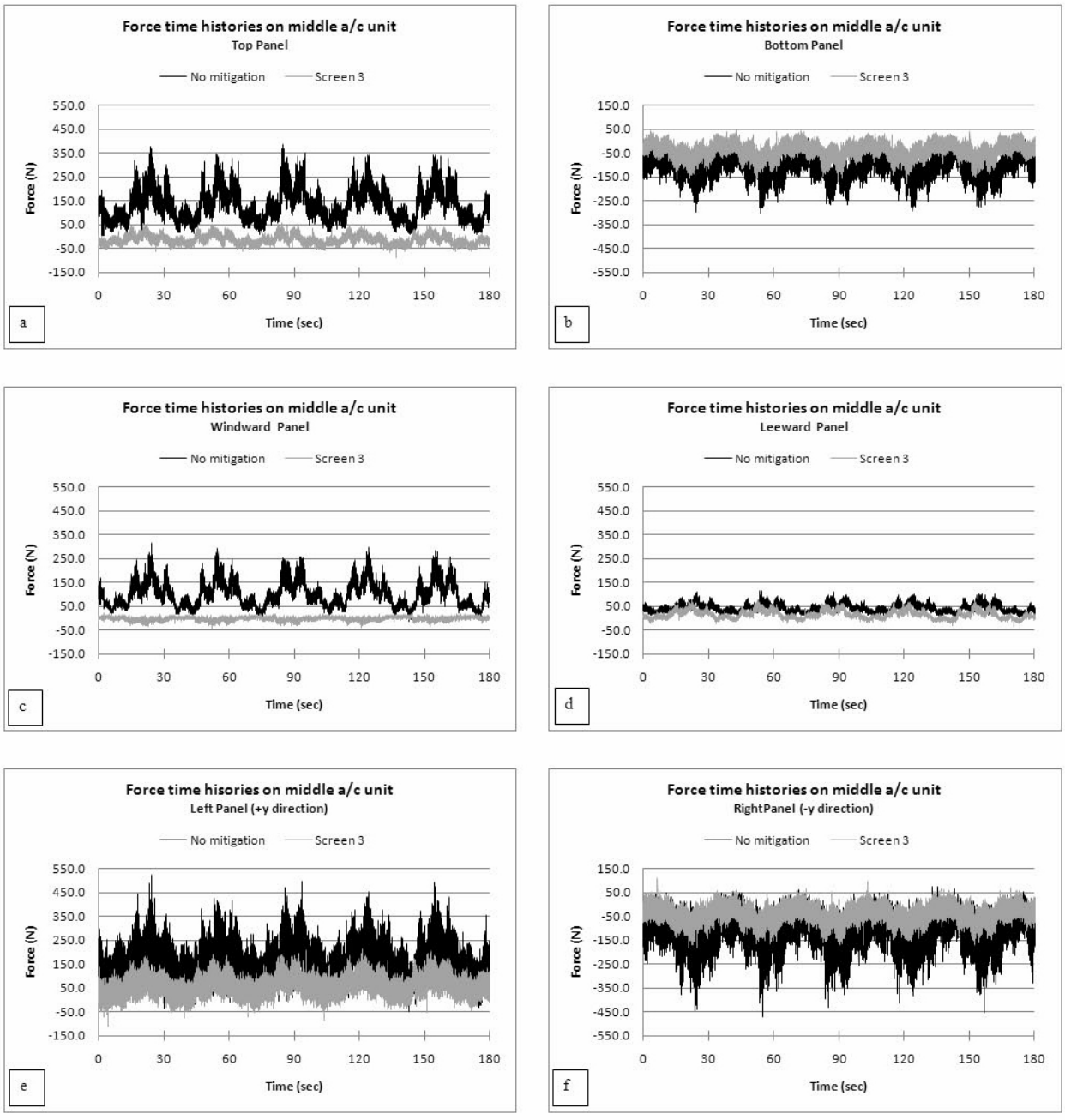

Fig. 10. Force time histories showing load reductions on each panel of the middle a/c unit during the screen 3 test: (a) top panel, (b) bottom panel, (c) windward panel, (d) leeward panel, (e) left panel, and (f) right panel.

Before the wind screen mitigation concept may be proven viable, more work is needed to investigate the effectiveness of the screens for a complete set of wind angles of attack, and for a variety of shapes and sizes of rooftop equipment. The mitigation device, itself, must not fail in hurricane winds. This study demonstrated that the wind screen was able to withstand the wind generated by the 6-fan WoW apparatus, representative of a Category 1 hurricane according to the Saffir-Simpson hurricane intensity scale (Huang et al., 2009). Further testing at higher sustained wind speeds is necessary to evaluate the performance of the wind screen under more intense hurricane conditions. Also, simultaneous measurements on the rooftop equipment and the screens will be desirable in order to evaluate the load distribution. Information of loading on the screens will be helpful to develop design provisions for their mounting mechanisms. Special attention should be paid in estimating loads on screens adjacent to the windward walls. Other design considerations for the wind screen should account for any necessary clearance requirements around the rooftop equipment, and should allow access to the equipment for routine inspection and maintenance. Last but not least, cost considerations may prove to govern the viability or otherwise of screens as a mitigation device.

Discussion of Code (ASCE 7-10) Provisions

The results of this study demonstrated that the peak lateral force coefficient of GC_f = 3.1 was approximately 50% higher than its wind tunnel counterpart of 2.1 (Hosoya et al., 2001), which dictates the lateral load prescribed in ASCE 7-10 Section 29.5.1. Thus, the ASCE 7-10 specified lateral loading could be non-conservative, having design implications that could lead to rooftop equipment detachment or failure during extreme winds. Future work is needed to evaluate the adequacy of current code provisions. In particular, testing is needed for a range of relative frontal areas and locations of the roof top equipment, considering various roof geometrical parameters and parapets.

Additionally, the ASCE 7-10 methodology for calculating rooftop equipment wind loading has some discrepancies with respect to building height (h), as it suggests using Eqns. 29.5-1 and 29.5-2 for $h > 18.3$ m (60 ft) and $h \leq 18.3$ m (60 ft), respectively. There are two problems with this: First, a vertical uplift force on rooftop equipment is accounted for buildings with h . 18.3 m (60 ft), however, not for buildings with $h > 18.3$ m (60 ft); Second, there will be an unrealistic difference in wind loads on rooftop equipment for two buildings with heights close to 18.3 m (60 ft), as demonstrated in the following example. Consider two rectangular office buildings, each having a flat roof and plan dimensions of 13.7 m × 13.7 m (45 ft × 45 ft), located in Iowa (basic wind speed = 51.4 m/s), and surrounded by flat terrain defined as Exposure B in all directions. One building has a height h = 18.3 m (60 ft), and the other has a height h = 19.1 m (62.5 ft). Both buildings have rooftop equipment with dimensions of $H \times L \times D = 0.73 \times 0.73 \times 0.73$ m (2.4 × 2.4 × 2.4 ft). Using ASCE 7-10 Eqn. 29.5-2, the rooftop equipment lateral and uplift wind loading for the building with h = 18.3 m (60 ft) were calculated as F_h = 1783.3 N (400.9 lb) and F_v = 995.5 N (223.8 lb), respectively. Using ASCE 7-10 Eqn. 29.5-1, a significantly lower wind loading of F_h = 806.9 N (181.4 lb) and F_v = 0 N (0 lb) were calculated for the slightly taller building having h = 19.05 m (62.5 ft). A uniform method for calculating rooftop equipment wind loading needs to be developed for buildings of all heights.

CONCLUSIONS

Wind loads exerted on full-scale representative rooftop equipment consisting of three a/c condenser units were measured. Probabilistic analyses of force measurements were performed based on observed time histories collected during the experiments. Significant overturning moments were observed in this study, but more work is needed to explicitly evaluate the overturning moment on different shapes, sizes, and configurations of rooftop equipment before design recommendations for overturning moment are proposed. The uplift force measured in a previous wind tunnel study is larger than the force measured in this study. The difference between the wind tunnel and the full-scale uplift forces may be attributed to the raised height of

the equipment on the a/c stand in the full-scale setup adopted in the present study. The lateral force coefficient was determined to be higher than the corresponding wind tunnel result. Comparison of load coefficients with those given in the ASCE 7 provisions suggests further work to be performed to evaluate the adequacy of current provisions.

Connection details can be strengthened to prevent rooftop equipment failure. However, this will not alleviate aerodynamic loading on the rooftop equipment panels and, therefore, not prevent panel failure under high winds. To reduce the wind loads acting on the rooftop equipment panels, a mitigation technique using wind screens was developed and tested for the a/c units. Comparative testing indicated that the presence of a porous metal screen installed around the full-scale rooftop equipment significantly reduced the aerodynamic loads on the equipment for each of the four screens tested. Screen 3 was found to be most effective, generating wind loading reductions on the rooftop equipment ranging from 56-69%. Results from the force and pressure studies suggest that the presence of a wind screen could alleviate the possible rooftop equipment failure modes identified in this study. Wind screen load reductions would decrease the likelihood of panels detaching from the a/c units, the a/c units detaching from the a/c stand, and the a/c stand detaching from the roof. Wind screens may also protect the rooftop equipment against flying debris, to an extent that has not been determined in this study.

The mitigation research described is this paper is preliminary and further work is needed to validate this technique and its cost-effectiveness. In addition, it would be beneficial to perform work using multi-axis load cells capable of directly measuring the simultaneous reaction forces and moments. Further study is needed to measure full-scale rooftop equipment wind loading at different wind angles of incidence, and to examine the wind loading across a broader range of full-scale rooftop equipment shapes, sizes, and types. Also, future work is needed to measure the reaction loads beneath mitigation devices such as the wind screens presented in this study. Future research on mitigation may also focus on designing rooftop equipment having more favorable aerodynamic shapes to alleviate wind loading as an alternative to the strengthening of the supporting structure and connections.

ACKNOWLEDGEMENTS

The 6-fan Wall of Wind was sponsored by RenaissanceRe Holdings Ltd. Wall of Wind research is supported by the National Science Foundation (NSF Award No. 0727871), Center of Excellence in Hurricane Damage Mitigation and Product Development, Florida Sea Grant College Program, Gulf of Mexico Regional Sea Grant Program, Florida Department of Emergency Management (FL DEM), Applied Insurance Research (AIR) Worldwide, the Roofing Industry Alliance for Progress, and others. Useful discussions with E. Simiu of the International Hurricane Center, FIU, are acknowledged with thanks. Assistance provided during the experiment by Mr. Walter Conklin and with data analyses by Mr. Ruilong Li, Ph.D. candidate at FIU, is greatly appreciated.

REFERENCES

1. Aly, A.M., Gan Chowdhury, A., Bitsuamlak, G. (2011), “Wind Profile Management and Blockage Assessment for a New 12-Fan Wall of Wind Facility at FIU.” Scheduled for publication (Vol.14, No.4, July, 2011), Wind and Structures.
2. American Society of Civil Engineers. ASCE 7-02, Minimum design loads for buildings and other structures, 2003.
3. American Society of Civil Engineers. ASCE 7-05, Minimum design loads for buildings and other structures, 2006.

4. American Society of Civil Engineers. ASCE 7-10, Minimum design loads for buildings and other structures, 2010.
5. Baker, C. J., (2007), "Wind engineering—past, present, and future," Journal of Wind Engineering and Industrial Aerodynamics; 95:843-70.
6. Bitsuamlak, G., Gan Chowdhury, A., Sambare, D., (2009), "Application of a full-scale testing facility for assessing wind-driven-rain intrusion," Building and Environment; 44 (12):2430-41.
7. Blessing, C., Gan Chowdhury, A., Lin, J., Huang, P., (2009), "Full-scale validation of vortex suppression techniques for mitigation of roof uplift," Engineering Structures; 31:2936-46.
8. Dagnew, A., Bitsuamlak, G., Gan Chowdhury, A. (2010). "Computational Blockage and Wind Simulator Proximity Effects Assessment for a New Full-Scale Testing Facility." Wind and Structures, 13 (1), pp. 21-36.
9. Dong, Z., Luo, W., Qian, G., Wang, H., (2007), "A wind tunnel simulation of the mean velocity fields behind upright porous fences," Agriculture and Forest Meteorology; 146:82-93.
10. Fang, F. M., Wang, D. Y., (1997), "On the flow around a vertical porous fence," Journal of Wind Engineering and Industrial Aerodynamics; 67-68:415-24.
11. Federal Emergency Management Agency. Mitigation assessment team report: Hurricane Charley in Florida. FEMA 488, 2005.
12. Federal Emergency Management Agency. Mitigation assessment team report: Hurricane Katrina in the Gulf Coast. FEMA 549, 2006.
13. Federal Emergency Management Agency. Summary report on building performance: 2004 hurricane season. FEMA 490, 2005.
14. Gan Chowdhury, A., Huang, P., Erwin, J., (2009), "Aerodynamic testing application of a full-scale facility for mitigating hurricane-induced coastal disasters," Far East Journal of Ocean Research, 2(1):1-27.
15. Gan Chowdhury, A., Simiu, E., Leatherman, S.P., (2009 α), "Destructive testing under simulated hurricane effects to promote hazard mitigation," ASCE Natural Hazards Review Journal, 10(1):1-10.
16. Gan Chowdhury, A., Aly, A.M., Bitsuamlak, G. (2010), "Full- and Large-Scale Testing to Promote Wind Disaster Mitigation." Proceedings of the Fifth U.S.-Japan Workshop on Wind Engineering (Chicago, Illinois, USA), p. 153-160.
17. Hosoya, N., Cermak, J.E., Steele, C. (2001), "A wind-tunnel study of a cubic rooftop ac unit on a low building," Americas Conference on Wind Engineering, p. 1-10 (CD-ROM).
18. Huang, P., Gan Chowdhury, A., Bitsuamlak, G., Liu, R., (2009), "Development of devices and methods for simulation of hurricane winds in a full-scale testing facility," Wind and Structures, 12:151-77.
19. Kang, J.H., Jo, Y.S., Cheon, I.K., Lee, S.J., (2007), "Experimental study on shelter effect of porous wind fences for reducing wind damage on kiwifruit plants," International Conference of Wind Engineering: Cairns, Australia, p. 2047-54.
20. Kopp, G.A., Bartlett, F.M., Galsworthy, J., Henderson, D., Hong, H.P., Inculet, D.R., Savory, E., St. Pierre, L.M., Surry, D., (2006), "The three little pigs full-scale testing facility." In: Proc. CSCE first specialty conference on disaster mitigation, DM-026-1-8.
21. Leatherman, S.P., Gan Chowdhury, A., Robertson, C.J., (2007), "Wall of wind full-scale destructive testing of coastal houses and hurricane damage mitigation," Journal of Coastal Research, 23(5):1211-7

22. Lee, S.J., Kim, H.B., (1999), "Laboratory measurements of velocity and turbulence field behind porous fence," Journal of Wind Engineering and Industrial Aerodynamics, 80:311- 26.

23. Lee, S.J., Park, C.W., (1998), "Surface-pressure variations on a triangular prism by porous fences in a simulated atmospheric boundary layer." Journal of Wind Engineering and Industrial Aerodynamics, 73:45-58.

24. Lopez, C., Masters, F., (2010), "Flow Measurement, Analysis and Simulation of Wind-Driven Rain for Engineering Applications." Proceedings of the 2nd Workshop of the American Association for Wind Engineering (AAWE) (Marco Island, Florida, USA), (CDROM).

25. Loredo-Souza, A.M., Schettini, E.B.C., Malcum, K.C., Guimaraes, A.F., Pimentel, J.L., Ignacio, L.R., (2007), "The effects caused by porous fences on the wind pressure distributions over a coal pile," International Conference of Wind Engineering: Cairns, Australia, p. 2023-30.

26. National Institute of Standards and Technology. "Performance of physical structures in Hurricane Katrina and Hurricane Rita: A reconaissance report," NIST Technical Note 1476, 2006.

27. Reinhold, T.A., (2006) "Wind loads and anchorage requirements for rooftop equipment," ASHRAE Journal, 48:37-43.

28. Sadek, F., Simiu, E., (2002), "Peak non-gaussian wind effects for database-assisted low-rise building design," Journal of Engineering Mechanics (ASCE), 128(5):530-9.

29. Santiago, J.L., Martin, F., Cuerva, A., Bezdenejnykh, N., Sanz-Andres, A., (2007), Experimental and numerical study of wind flow behind windbreaks." Atmospheric Environment, 41:6406-20.

30. Smith, J., Masters, F.J., (2010), "Validation of Facility Configuration and Investigation of Control Systems for the 1:10 Scaled Insurance Center for Building Safety Research." Proceedings of the 2nd Workshop of the American Association for Wind Engineering (AAWE) (Marco Island, Florida, USA), (CD-ROM).

31. Yaragal, S.C., Govinda Ram, H.S., Murphy, K.K., (1997), "An experimental investigation of flow fields downstream of solid and porous fences," Journal of Wind Engineering and Industrial Aerodynamics, 66:127-40.

32. Yu, B., (2007) "Surface mean flow and turbulence structure in tropical cyclone winds," Ph.D. dissertation. Florida International University: Miami, FL, USA.

33. Yu, B., Gan Chowdhury, A., (2009), "Gust factors and turbulence intensities for the tropical cyclone environment," Journal of Applied Meteorology and Climatology, 48(3):534-52.

34. Yu, B., Gan Chowdhury, A., Masters, F.J., (2008) "Hurricane power spectra, co-spectra, and integral length scales," Boundary Layer Meteorology, 129:411-30.

ABOUT THE JOURNAL

Aims

The aim of the Journal is a continuous and timely dissemination of research developments and applications. The Journal is an inter disciplinary forum for Wind and Engineering and publishes referred papers on the latest advances on the subject and their application to industrial wind engineering, wind induced disasters, environmental issues and wind energy. Papers on relevant and innovative practice and engineering application as well as those of an interdisciplinary nature are strongly encouraged. Discussions on any paper previously published in the Journal are also considered for publication. Articles submitted to the Journal should be original and should not be under consideration for publication elsewhere at the same time.

Besides regular issues containing contributed research papers, it will be the endeavour of the editors to bring out specialty issues covering a specific area of interest to include invited state-of-the-art papers.

Furthermore, short technical notes describing preliminary ideas on a proposed area of future research will also be considered for publication.

Members may also send news items, memoirs, book reviews for publication.

The Society is not responsible for statements and opinions expressed by the authors in the Journal.

Subscription

The journal will be brought out biannually. For ISWE members, subscription to ISWE Journal is included in the membership fee. Hard copies will be sent only on request on first come first served basis.

The rates per issue for non-members are given below :

Regular Issue	: Rs. 300.00 (US$ 50.00, by air mail)
Special Issue	: Rs. 1000.00 (US$ 100.00, by air mail)
Library Membership (Annual)	: Rs. 2000.00 (US $ 200.00 by air mail)

There are no page charges for the Journal of Wind and Engineering.
A copy of the journal will be sent by post to all corresponding authors after publication. Additional copies of the journal can be purchased at the author's preferential rate of Rs. 300.00 per Volume.

Preparation of the Manuscript

a. **Paper Length** : The length of paper should normally be restricted to 10 pages maximum.

b. **Headings and subheadings** : Headings should be in bold uppercase and not numbered. Sub- headings should be in bold lower case and may be numbered.

c. **Figures and Tables**: These should be numbered consecutively in Arabic numerals and should be titled. Figure captions should be given on a separate sheet. Figures should be very sharp. Scanned figures shall not be accepted.

d. **Photographs, Illustrations**: Good glossy bromide prints of these must accompany the manuscript and not be attached to the manuscript pages.

e. **References**: These should be listed alphabetically at the end of the text and numbered serially, cited in the text by the last name(s) of authors followed by the year of publication in parenthesis. In case of more than two authors, the last name of the first author followed by et al. and the year of publication is to be cited in the text. References are to be listed in he following format only:

1. Walker, G.R., Roy, R.J. 1985. Wind loads on houses in urban environment. Proc. of Asia Pacific Sym. on Wind Engg., University of Roorkee, Roorkee, India, Dec. 5-7.
2. Holmes, J.D., Melbourne, W.H. and Walker, G.R. A commentary on the Australian Standard for wind loads. Australian Wind Engineering Society, 1990.
3. Krishna, P., Kumar, K., Bhandari, N.M., (2005), "Review of Wind Loading Codes", A study sponsored by Gujarat State Disaster Management Authority, India.

f. **Abstract**: This should not exceed 150 words and be an abbreviated, accurate representation of the contents of the article. It should be followed by a list of 3 to 5 key words of these contents.

g. **Units**: All quantities should be in SI units. Other units may be enclosed in parenthesis after the SI units, if necessary.

Submission

Manuscript of the paper should be transmitted by e-mail, or, alternatively, the original manuscript together with a soft copy on CD should be submitted to the Editor-in-Chief / Editors for possible publication in the Journal.

Please make sure your contact address is clearly visible on the outside of all packages you are sending to the Editors.

Editorial Office: Located at : Office of Dr. Achal Kumar Mittal, Scientist
Central Building Research Institute
Roorkee - 247667, INDIA, Tel: 01332- 283464
E-mail: iswe1993@gmail.com; achal_cbri@rediffmail.com
http://www.iswe.co.in

All enquiries may be addressed to the Editor-in-Chief / Editors Hon. Secretary, at this address.

Submitting a Paper to Journal

1. In order to maintain annonymity during any referring process, authors are requested to refrain from, or keep to a minimum, self-referencing.

2. In consideration of the publication of your Article, you assign us with full title guarantee, all rights of copyright and related rights in your Article. So that there is no doubt. This assignment includes the right to publish the Article in all forms, including electronic and digital forms, for the full legal term of the copyright and any extension or renewals. You shall retain the right to use the substances of the above work in future works, including lectures, press releases and reviews, provided that you acknowledge its priorpublication in the Journal.

3. We shall prepare and publish your Article in the journal. We reserve the right to make such editorial changes as may be necessary to make the article suitable for publication; and we reserve the right not to proceed with publication for whatever reason. In such an instance, copyright in the Article will revert to you.

4. You hereby assert your moral rights to be identified as the author of the Article according to the Indian Copyright Designs & Patents Act.

5. You warrant that you have secured the necessary written permission from the appropriate copyright owner or authorities for the reproduction in the Article and the Journal of any text, illustration, or other material. You warrant that, apart from any such third party copyright material included in the Article, the Article is you original work, and cannot be construed as plagiarizing any other published work, and has not been and will not be published elsewhere.

6. In addition, you warrant that the Article contains no statement that is abusive, defamatory, libelous, obscene, fraudulent, nor in any way infringes the rights of others, nor is in any way unlawful or in violation of applicable laws.

7. You warrant that, wherever possible and appropriate, client or participant mentioned in the text has given informed consent to the inclusion of material pertaining to themselves, and that they acknowledge that they cannot be identified via the text.

8. If the Article was prepared jointly with other authors, you warrant that you have been authorized by all co-authors to sign this Agreement on their behalf, and to agree on their behalf the order of names in the publication of the Article.

OBJECTIVES OF THE INDIAN SOCIETY FOR WIND ENGINEERING

(a) The Society shall provide a necessary forum to the individuals and institutions connected with, or, interested in industrial aerodynamics, which includes wind effects on structures and buildings, land and sea transportation vehicles; mitigation of disasters due to cyclones, tornadoes, blizzards, sand storms, etc.; wind energy generation; study of atmospheric pollution and dispersion; and, related matters to come together and exchange ideas for the advancement and dissemination of knowledge in the field of Wind Engineering

(b) The Society shall promote research and development work in the field of Wind Engineering and shall maintain close liaison with the International Organizations working with allied objectives.

(c) The Society shall promote research results in professional practice.

(d) The Society shall make efforts to involve field engineers and professional organizations in its activities by arranging seminars, symposia, etc.

(e) The Society shall bring out a periodical publication.

(f) The Society shall institute awards and prizes to recognize excellence of research and application in Wind Engineering.

MEMBERSHIP OF THE SOCIETY

The Society shall have the following categories of membership:

(a) Individual (b) Institutional
(c) Honorary

Subscription: The life membership rates for different categories shall be as follows:

Individual Membership			
Indians and SAARC Nationals	Life	Rs.	1500.00
Other Foreign Nationals	Life	US$	100.00
Institutional Membership	Annual	Rs.	3,000.00
	Regular	Rs.	30,000.00

ISWE EXECUTIVE COMMITTEE

President	Dr. P. D. Porey	Director SVNIT, Surat
Vice-President	Dr. S. Arunachalam	Director Grade Scientist, SERC Chennai
Hon. Secretary	Dr. Achal Kumar Mittal	Scientist CBRI, Roorkee
Treasurer	Dr. Akhil Upadhyay	Asso. Prof. IIT, Roorkee
Members	Sh. T. N. Gupta	Former Executive Director, BMTPC Delhi
	Dr. G. S. Mandal	NDMA, Delhi
	Dr. Abhay Gupta	VP, Eigen, Noida
	Sh. Deepak Bansal	Asstt. Chief Projects, HUDCO, Delhi
	Dr. O. R. Jaiswal Asso.	Prof VNIT, Nagpur
	Sh. Ashok Kumar J. Shah	Prof. SVNIT, Surat
	Dr. (Mrs.) S. Selvi Rajan	Dy. Director, SERC Chennai
	Sh. Sanjay Kumar Varsheny	GM, Mahagun, Delhi

COMMUNICATION

Communication regarding change of address, subscription renewals, missed numbers, membership and Society Publications should be addressed to -

Dr. Achal Kumar Mittal
Hon. Secretary
Indian Society for Wind Engineering,
Located at the Central Building Research Institute
Roorkee - 247667, INDIA
Tel: 01332- 283464
Mob: +91 9412074408
E-mail: iswe1993@gmail.com, achal_cbri@rediffmail.com
http://www.iswe.co.in

ISSN : 0973 - 0613

JOURNAL OF WIND & ENGINEERING

Vol. 8 No. 1 January 2011

CONTENTS

Published by: Indian Society for Wind Engineering, Located at Central Building Research Institute Roorkee 247667, INDIA, Tel: 01332- 283464, E-mail: iswe1993@gmail.com,http://www.iswe.co.in

Printed by : *R. K. Printers & Publishers, 26 Civil Lines, New Haridwar Road, Roorkee - 247667 Ph. : 270957, 9897276995*